2. Infrared (IR) Spectroscopy

2.1. Introduction

Infrared spectroscopy is an absorption method in the wavelength region of 1 to 100 μm in that extends the region of the visible light to longer wavelengths and smaller frequencies/energies. The energy of infrared light is no longer sufficient to induce transitions of valence electrons. Instead, infrared radiation excites vibrational and rotational motions in molecules. Except for the differences in the energy transfer from the radiation to the molecule, the principles of IR spectroscopy are the same as those of VIS/UV spectroscopy or other spectroscopic techniques. The absorption of infrared light is again characterized by the Bouger-Lambert-Beer Law.
However, infrared spectra are usually presented by a plot of the percentage of transmission vs the wavenumber in cm^{-1} (as opposed to a plot of absorbance vs. the wavelength in nm in UV/VIS spectroscopy). A typical IR spectrum is therefore recorded from about 4 000 to 10 000 cm^{-1} (upper limit) to about 100-800 cm^{-1} (lower limit).

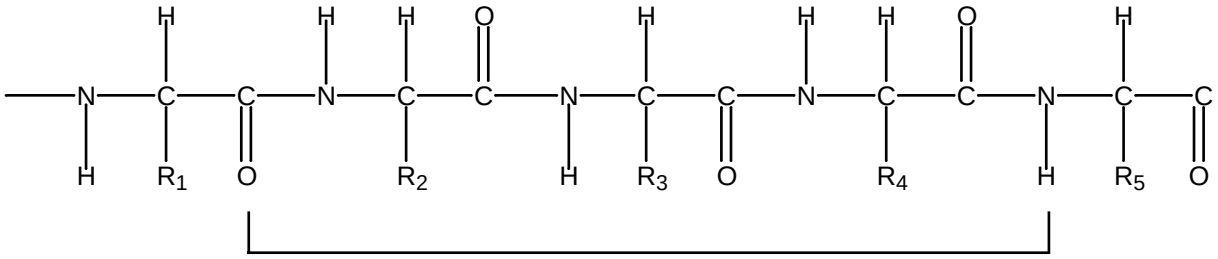

Figure 2.1 In an α-helix the hydrogen bond is formed between the carbonyl group of residue n and the amide nitrogen of residue n+4

What information can be deduced by IR spectroscopy from biological samples ?
As an example for the utility of Infrared spectroscopy in biology, the amide bond can be used to identify protein secondary structure. *Figure 2.1* shows a sequence of the polypeptide chain of proteins. This sequence can lead to different types of a secondary structure, for example α-helix and β-sheet, which were correctly predicted by Corey and Pauling (Figure 2.2) using theoretical considerations before these structural elements were found experimentally.

Linus Pauling and Robert Corey with model molecule

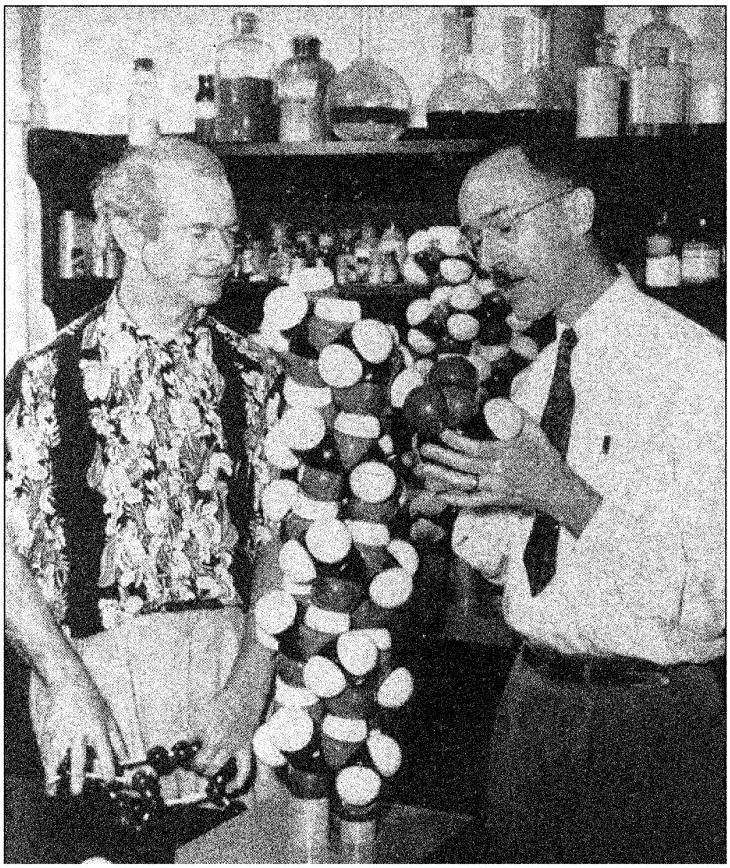

Figure 2.2 Linus Pauling and Robert Corey with model molecule

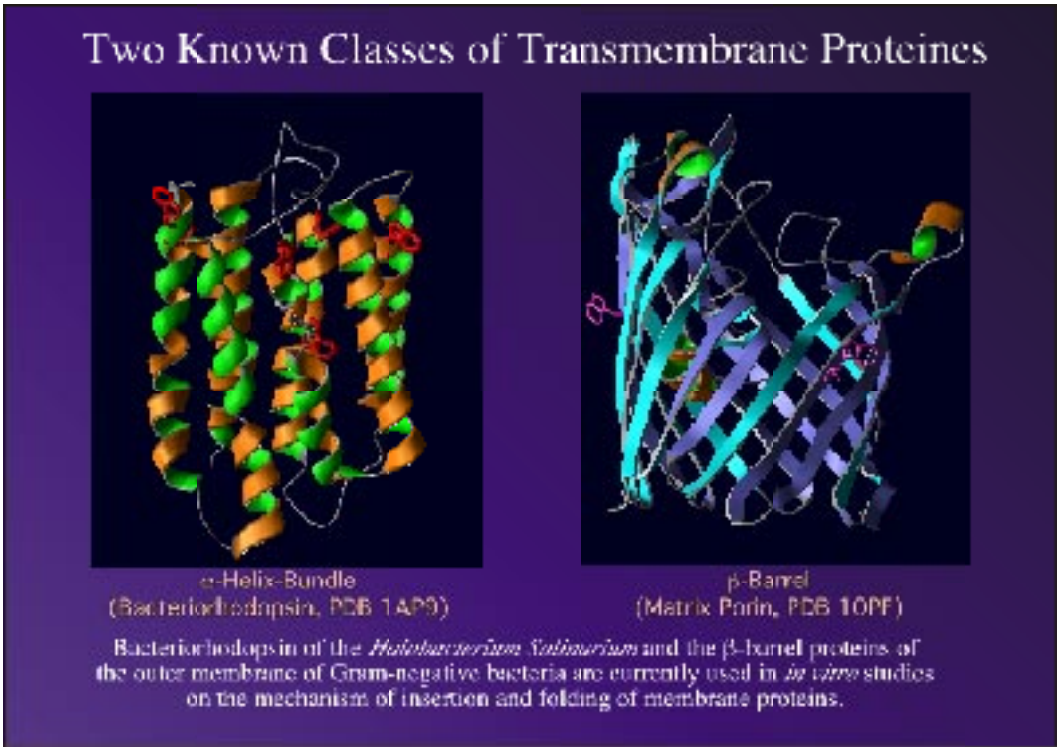

Figure 2.3 Two known structural motives of transmembrane domains of membrane proteins

Figure 2.3 shows the ribbon structures of two membrane proteins that illustrate protein secondary structure, that of the seven helix bundle protein bacteriorhodopsin from halobium salinarium and that of the matrix porin. While these structures have been determined by x-ray crystallography on solid protein crystals, spectroscopic methods can be used to determine structural elements of proteins in aqueous solution. These methods have proven to be very useful to quickly elucidate the secondary structure of a protein and to determine, whether there are changes in the secondary structure when the protein interacts with other molecules.

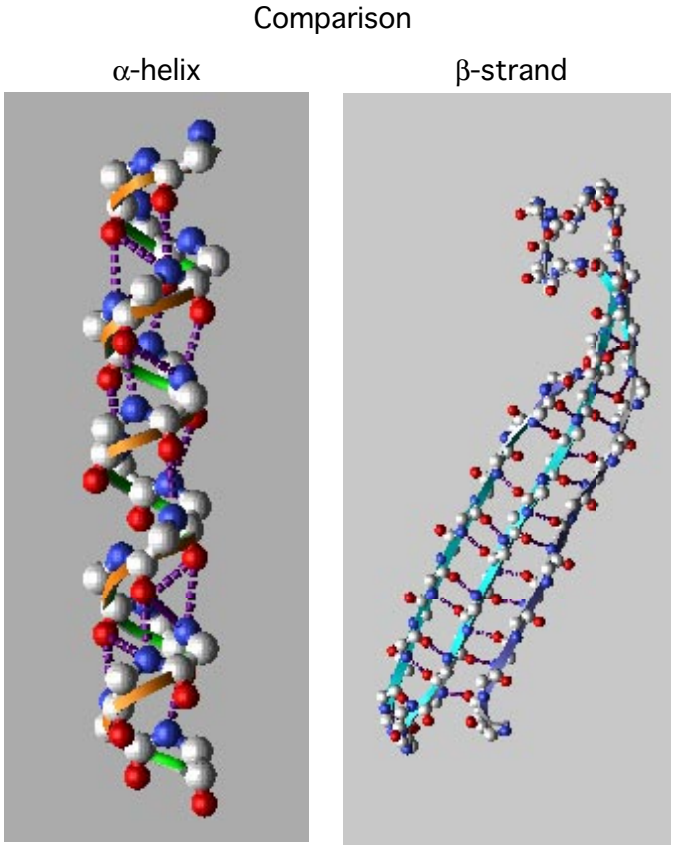

Figure 2.4 Comparison of the hydrogen bonding patterns in α-helices and antiparallel β-strands

While solution NMR-spectroscopy provides a detailed image of the structure of a protein, the NMR method is much more complex and requires a time investment of many months to several years. The NMR spectroscopists need large quantities of proteins that have to be labeled by isotopes of carbon (^{13}C), nitrogen (^{15}N), oxygen (^{17}O, and hydrogen (^{2}H). By contrast, FT-IR spectroscopy results in secondary structure information within hours or days. In addition, modern IR spectroscopy is suitable in time resolved experiments to monitor changes in secondary structure in protein folding experiments or in studies on protein function. IR spectroscopy can be applied to very large proteins, while solution NMR methods to solve the protein structures of molecules larger than 20 kDa are still in development. Structure determination by crystallography requires protein crystals and crystallization of proteins is also a time consuming task, that may often take months to years to complete. However,

crystallography is not limited by the size of the protein and usually gives high resolution details of the atomic structure of the protein in a crystal. The different methods thus suit different needs in the investigation of biological systems.

α-helices (Figure 2.4) are characterized by a rod-like structure in which the polypeptide main chain is tightly coiled and forms the inner part of the rod, whereas the side chains extend outward in an helical array. The α-helix is stabilized by hydrogen bonds between the NH and CO groups of the main chain. The CO group of each amino acid is hydrogen bonded to the NH group of the amino acid that is four residues ahead in the linear sequence. Thus, all the main chain CO and NH groups are hydrogen bonded. 3.6 residues are required for one full turn of the peptide backbone. Thus the angle between two amino acids is 100 ° and their distance projected to the helix axis is 1.5 Å (10^{-10} m), resulting in a displacement of 5.4 Å per turn along the helix axis. β-strands are different from α-helices: they do not form rods but sheets. A so-called β-pleated sheet or β-strand is almost fully extended rather than being tightly coiled as in the α-helix. The axial distance between adjacent amino acids is 3.5 Å in contrast to 1.5 Å for the helix. Another difference is that the β-pleated sheet or β-strand is stabilized by hydrogen bonds between NH and CO groups in different polypeptide chains, whereas in the α-helix the hydrogen bonds are between NH and CO groups in the same polypeptide chain. Adjacent chains can be either parallel, i.e. they are oriented in the same direction, or antiparallel, i.e. they run in opposite directions. The reversal of the direction of the polypeptide chain between two β-strands is called a β-turn (also known as a reverse turn or a hairpin bend).

2.2. Relation between protein secondary structure and infrared absorption.

In peptides and proteins there are three absorption bands that are of particular importance. The amide A Band at 3300 cm^{-1} that characterizes the N-H-stretch vibration, the amide I band at 1650 cm^{-1} that characterizes the C=O -stretch vibration and the amide II band at 1550 cm^{-1} that characterizes the N-H bending vibration. These 3 oscillations belong to the backbone of the polypeptide chain and are therefore relatively intense. These vibrations are not independent of each other. Because of the formation of particular hydrogen bonding patterns in the peptide sequences of the protein that form secondary structures, they are coupled oscillators. In α-helices or β-strands (see figure of secondary structures with hydrogen bonds displayed as dotted lines) the coupling of these oscillators is different and therefore the infrared spectra of a protein are dependent on its secondary structure.
The infrared spectra of poly-L-lysine shall serve as an example for the spectral features peptides that may exist in different conformations, depending on the environment of the

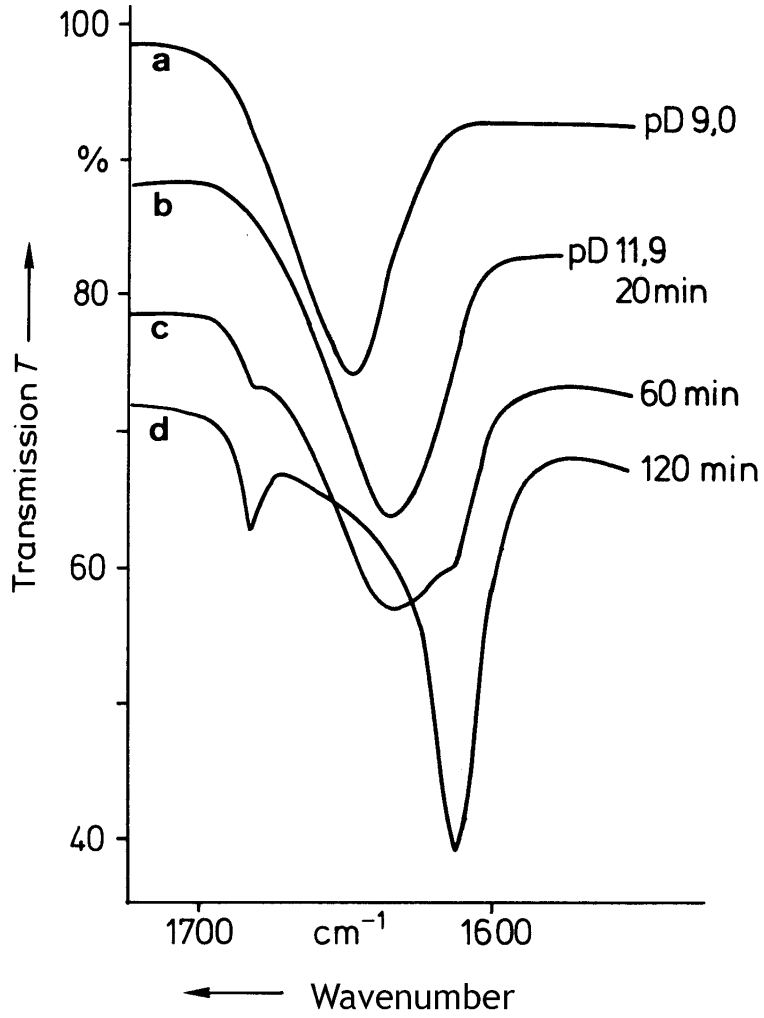

Shift of the amide-I band of polylysine in D_2O:
a, random coil at pD 9
b, a-helix at pD 11.9 after 20 min
c, transition to β-sheet after 1 h
d, fully formed β-sheet after 2 h.

(after Susi, H., J. Biol. Chem. 242, 1967)

Figure 2.5 Amide I absorption band of polylysine in D2O at different conditions.

peptide. The amide I band, which is observed at 1700 cm^{-1} for a free C=O vibration, is observed at 1655 cm^{-1} for a random coil structure and at 1650 cm^{-1} in the a-helical conformation. After a transition induced by high pH, the amid I band is split into a weak band at 1690 cm^{-1} and a strong band at 1620 cm^{-1}. The strong difference between absorption bands that are characteristic for different protein conformations can also be observed in biologically relevant peptides and proteins. Table 2.1 below summarizes the characteristic frequencies of the amide I, the amide II, and the amide A band.

Position of the amide bands depending on the secondary structure of the protein or peptide:

Konformation	Vibration frequency, ν (cm^{-1}) Amide A (N-H stretch)	Amide I (C=O stretch)	Amide II (N-H deformation)
α-helix	3290-3300	1648-1660	1540-1550
β-sheet	3280-3300	1625-1640 (strong) 1690 (weak)	1520-1530
β-turns		1660-1685	
random coil (unordered, non-hydrogen -bonded)	3250	1652-1660 (deuterated 1640-1648)	1520-1545
3_{10}-helix		1660-1670	
aggregated strands		1610-1628	

Sources: Tamm, L.K. and Tatulian, S. A., Infrared Spectroscopy of Proteins and Peptides in Lipid Bilayers, Quarterly Reviews of Biophysics, Nov. 1997

Cantor and Schimmel: Biophysical Chemistry, Part II, Freeman and Company, 1980

Table 2.1 Amide I wavenumbers and protein secondary structure.

Based on these relations between secondary structure and IR absorption frequencies, the structural components of proteins may be determined.

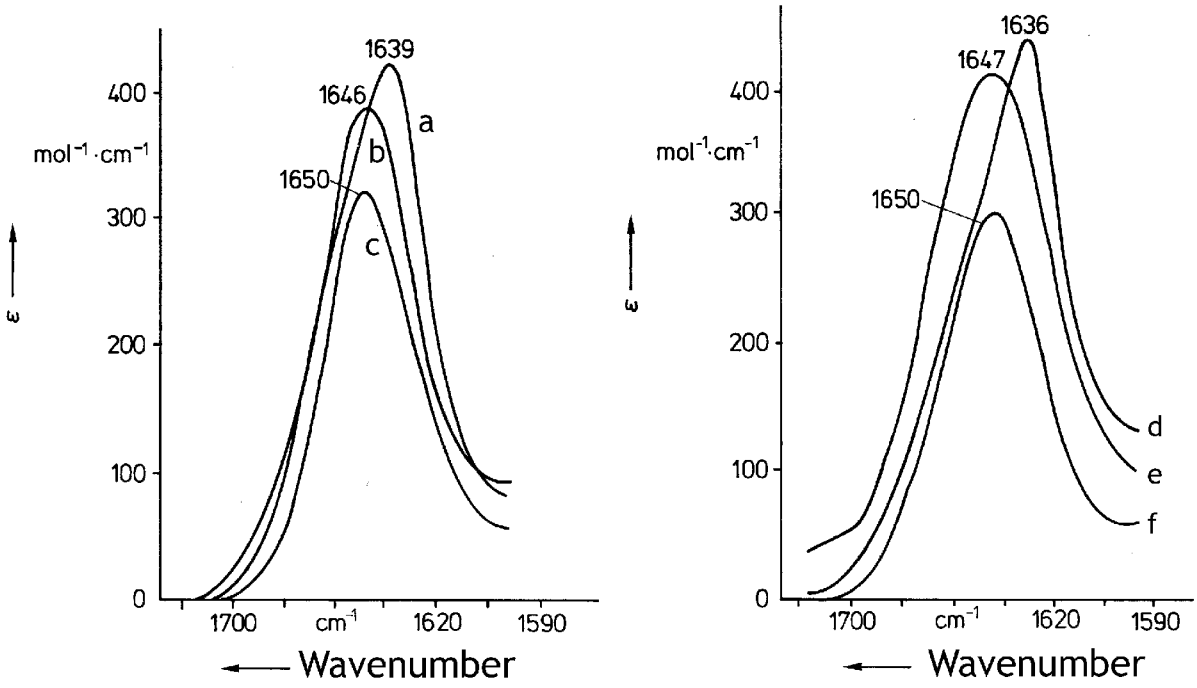

IR-absorption spectra of proteins around 1650 cm^{-1}

a, Ribonuclease; b, Lysozyme; c, Cytochrome c; d, Concavaline A; e, Insuline; f, Methemoglobine. After K. Ekkert et al., Biopolymers 16, 2549, (1977).

Figure 2.6 IR spectra of various proteins

Percentage of secondary structures, a-helices, β-strands, and random coils of 6 proteins and the position of the maximum of the infrared absorption band at 1650 cm^{-1}.

	PROTEIN	β-STRAND	α-Helix	random coil	λ_{max} (cm^{-1})
f	Methemoglobine	0	71	29	1650
e	Insuline	24	49	27	1647
c	Cytochrome c	0	39	61	1650
b	Lysozyme	10	35	55	1646
a	Ribonuclease	36	12	52	1639
d	Concavaline A	38	2	60	1636

Table 2.2 Percentages of secondary structure in various proteins determined by IR spectroscopy

The proteins are given in the sequence of decreasing α-helical content. The largest fraction of α-helical secondary structure is observed on methemoglobin. The maximum of the IR absorption band is found at 1650 cm^{-1}. In contrast, proteins such as concavaline A or Ribonuclease, with a higher content of β-sheet secondary structure have an absorption band with a maximum at 1636 cm^{-1}.

2.3. How is the composition of secondary structure determined ?

Infrared absorption bands are broad and often overlap with neighboring bands to produce a complex absorption profile. To elucidate the structural components of the protein, it is necessary to determine the component bands that overlap and generate the composite spectrum. The amide I band is most often subject to such an analysis of secondary structure. Two resolution enhancement techniques, differentiation and Fourier self-deconvolution, are commonly used to identify the component bands. Both methods do not increase instrumental resolution, but are mathematical procedures that yield narrower component bands.

Although in many cases deconvolved amide I bands have been used to determine secondary structure by curve fitting, it should be recognized that resolution enhanced spectra, especially derivative spectra do not reproduce true band intensities and relative component fractions cannot be obtained directly from them. Finally, noise is enhanced in these spectra, which, depending on initial data quality, puts a limit on the extent to which resolution can be enhanced. Despite these shortcomings, both methods are extremely useful for identifying component frequencies in complex spectra and these band positions can then be used as fixed input parameters in component band-fitting routines on the original unprocessed spectra. Before these techniques are applied, peaks due to residual water vapor must be carefully subtracted from the raw spectra, because spurious spectral contaminants like those from water vapor will also be enhanced by these methods. The sharp peaks of water vapor can be reliably subtracted by inspecting the amide I region (~1650 cm^{-1}) of the spectrum. When H_2O (in contrast to D_2O) buffers are used and an analysis of the amide I band is attempted, the spectral region around 2125 cm^{-1} is well suited to check for the correct subtraction of liquid water because this region is usually free from protein and lipid absorbance. In some cases a complete subtraction of the water bands is not possible because water bound to proteins can exhibit altered band shapes.

2.4. Principles of molecular vibrations. The harmonic oscillator.

Before more applications of infrared spectroscopy are discussed, the basic principles of infrared spectroscopy shall be explained.

Vibrational transitions in a molecule occur between distinct vibrational energy levels. Intramolecular vibrations and intermolecular vibrations are contributing to the spectrum. The simplest possible situation is a vibration between two atoms of a diatomic molecule. The atoms are located at an average internuclear distance r , the bond length. An attempt to squeeze the atoms more closely together will lead to a rapid increase of the repulsive force between the two atoms. An attempt to pull them apart is resisted by the attractive force. Both displacements require an input of energy which can be described as a function of the distance between the two atoms.

Model of an oscillating diatomic molecule vibrating around an equilibrium distance r_0

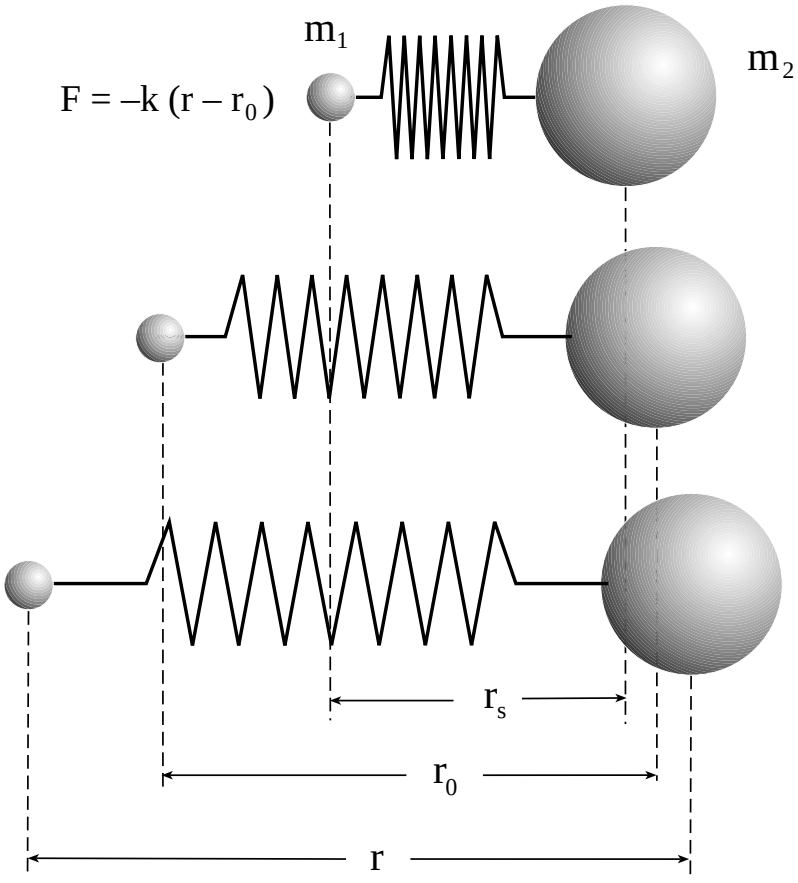

Figure 2.7 Oscillation of a diatomic molecule around an equilibrium distance.

We assume that the molecular bond between two atoms is comparable to a spring between

two spheres of the masses m_1 and m_2. The force of compression or expansion is then given by Hook's law:

$$F = -k(r - r_0)$$

k is a constant, $r\text{-}r_0$ the distance difference to the equilibrium distance generated by the force (F). The force is directed against the displacement of the atoms and thus has a negative sign. The potential energy of the oscillating system

$$E = \frac{1}{2}k(r - r_0)^2$$

increases symmetrically when the distance between both atoms is decreased or increased compared to the equilibrium distance.

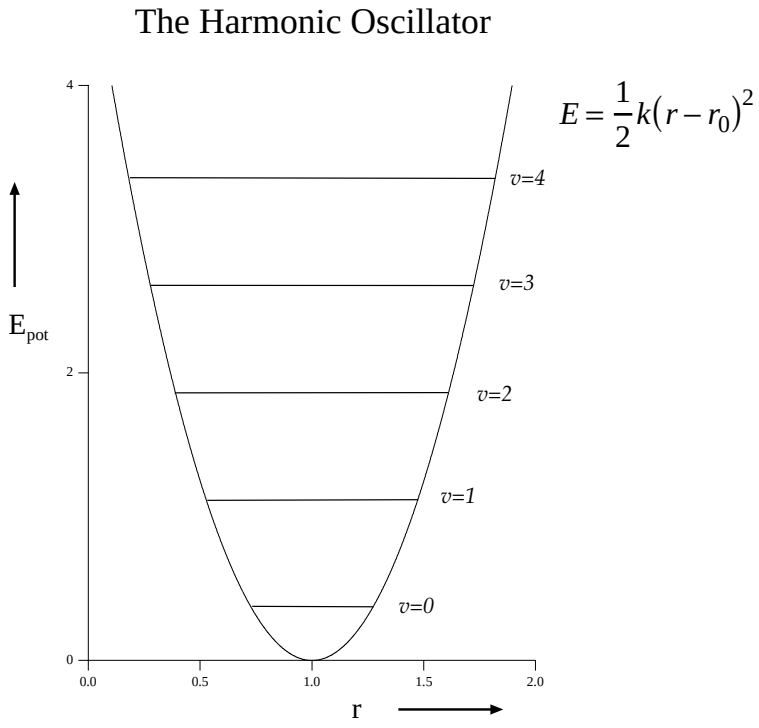

Figure 2.8 Potential energy as a function of distance in a harmonic oscillator

The vibration of such a diatomic molecule is characterized by an oscillation frequency that is given by classical mechanics:

$$\nu_{vib} = \frac{1}{2\pi}\sqrt{\frac{k}{\mu}}$$

where μ is the reduced mass of the system:

$$\mu = \frac{m_1 \cdot m_2}{m_1 + m_2}$$

Thus, the oscillation frequency is only dependent on the force constant (k) and on the masses of the oscillating atoms. The larger the mass of an atom, the smaller the frequency (wavenumber) of the vibration. The amplitude of the vibration has no effect on the frequency.

In contrast to classical mechanics, vibrational energies of molecules are quantized like all other molecular energies. The allowed vibrational energies are

$$E_v = \left(v + \frac{1}{2} \right) h\nu_{vib}$$

where v is called the vibrational quantum number. The equation implies that the lowest vibrational energy (i.e. for v=0) is E = 1/2 hν. The implication is that a molecule can never have zero vibrational energy; the atoms can never be without a vibrational motion. The quantity E = 1/2 hν is known as the zero-point energy, that depends on the classical oscillation frequency and hence on the strength of the chemical bond and on the masses of atoms that participate in this bond.

Further use of the quantum mechanics leads to a simple selection rule for the harmonic oscillator undergoing vibrational changes:

$$\Delta v = \pm 1$$

In addition to this selection rule the condition must be fulfilled that vibrational energy changes will only be observed in a spectrum if the vibration energy can interact with radiation, i.e. if the dipole moment of the molecule is changing with the vibration. Thus infrared spectra can be observed only in heteronuclear diatomic molecules, since homonuclear diatomic molecules have no dipole moment.

The energy of a transition between two vibrational states is then given by

$$E_{v+1} - E_v = \left(v + 1 + \frac{1}{2} \right) h\nu - \left(v + \frac{1}{2} \right) h\nu = h\nu$$

To have resonance between the vibrating molecule and the exciting radiation, the frequency of the radiation must be identical to the frequency of the vibration.

2.5. The anharmonic oscillator

Molecules do not exactly behave like to masses that are connected by a spring and described by the harmonic motion. Real bonds are elastic, but do not obey Hook's law. Bonds can break if they are stretch beyond a limiting distance and the molecule will dissociate. For amplitudes that exceed a certain value, the vibration must be described differently. A purely empiric description of such a behavior was derived by P.M. Morse and is called the Morse function.

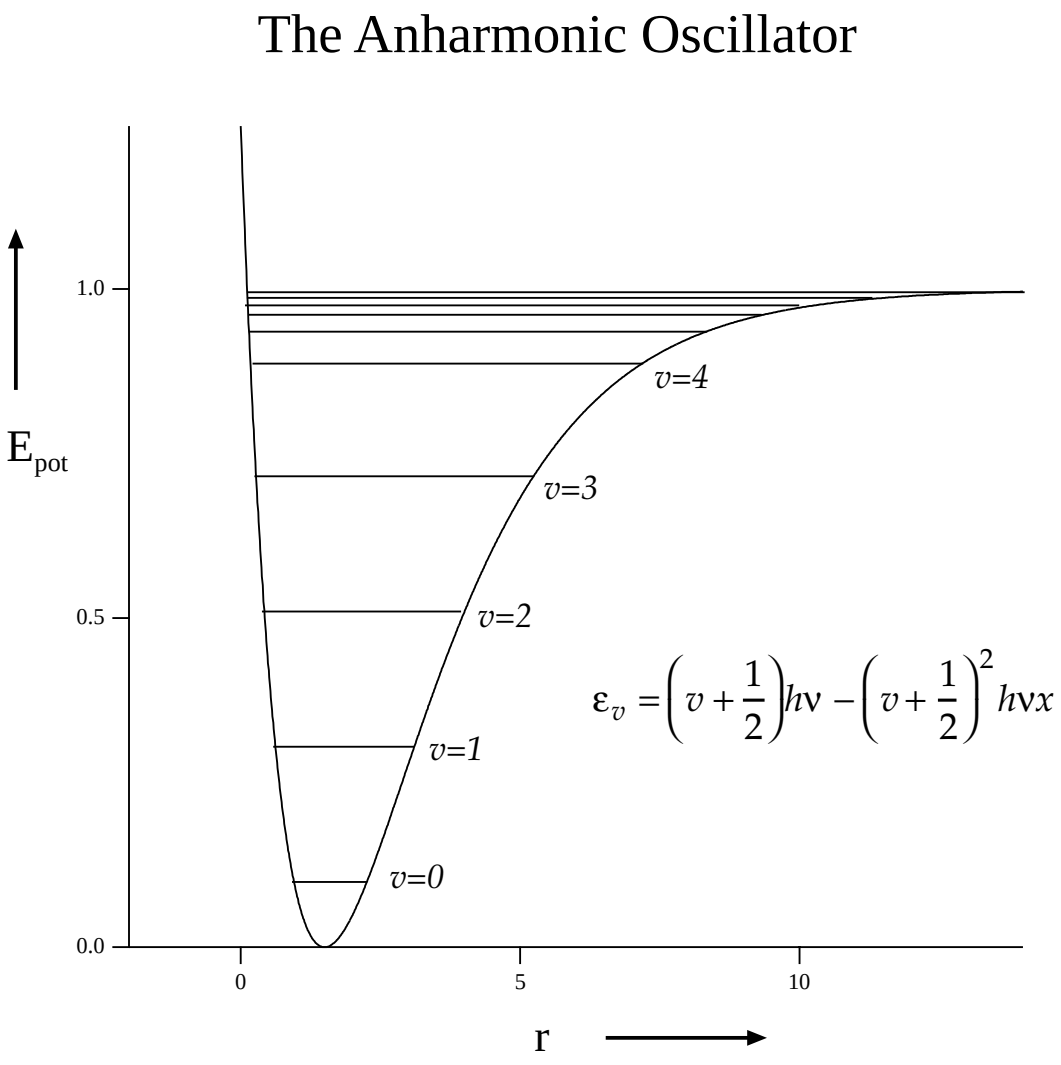

$$E = D_{Min}[1 - \exp\{-a\,(r-r_0)\}]^2$$

Morse Function, after P.M. Morse

Figure 2.9 The potential energy of the anharmonic oscillator is described by a Morse function (Morse potential).

In the Morse function, a is a constant for a particular bond and D_{min} is the dissociation energy. If the Morse function is used instead of the energy of the harmonic oscillator to derive the discrete energy levels, that are given by

$$\varepsilon_v = \left(v + \frac{1}{2}\right)h\nu - \left(v + \frac{1}{2}\right)^2 h\nu x$$

where x is an anharmonicity constant, that is small for bonding vibrations and always positive. Again, the Morse function is approximation and more accurate descriptions require additional cubic and terms of higher order with additional anharmonicity constants. The magnitude of these additional anharmonicity constants is rapidly getting smaller with increased order of the anharmonicity term. The selection rules for the anharmonic oscillator are

$$\Delta v = \pm 1,\ \pm 2,\ \pm 3,\ \ldots$$

Thus they are the same as for the harmonic oscillator, with the additional possibility of larger jumps. However the intensity of the resonance line decreases strongly with the difference in the energy levels and transitions with $\Delta v = \pm 3$ or higher are only rarely observed.

2.6. Vibrational Degrees of Freedom

A molecule with N atoms can be described by the locations of each atom in space by three coordinates, x, y, z. The total number of such coordinates is therefore 3 N. The molecule has 3N degrees of freedom. In such a description, the position of the molecule and the bond-angles are fixed. The translation of the molecule in space is described by three degrees of translational freedom. For the rotational motion of a nonlinear molecule we need additional three degrees of freedom, for a linear molecule just two (the rotation around the bond axis of a linear molecule does not result in a change of the coordinates of the atoms). Therefore, a non-linear molecule must have

3N-3-3 = 3N-6	(non-linear molecule)
3N-3-2 = 3N-5	(linear molecule)

degrees of freedom of internal vibration. A molecule like CO_2 therefore has 4 vibrational degrees of freedom, whereas H_2O has only 3 vibrational degrees of freedom. The number of vibrations derived in this way is called the number of fundamental vibrations or the normal modes of vibration or plain the normal vibrations.

The vibrations are classified in symmetrical and asymmetrical vibrations, depending on the maintenance of symmetry in the molecule. One further differentiates between vibrations along the atom bond, which are called valence or stretching vibrations (symbol ν) and

vibrations that change the shape of the molecule. The latter vibrations are called deformation vibrations (symbol δ). Both valence and deformation vibrations can be symmetric or asymmetric and therefore the change in the symmetry of the vibration is added as an index:

symmetric valence (stretching) vibrations: v_s (see transparency)
asymmetric valence (stretching) vibrations: v_{as}
symmetric deformation (bending) vibrations: d_s
asymmetric deformation (bending) vibrations: d_{as}

Deformation vibrations can either take place in the plane that is spanned by the three atoms or out of this plane. Typical vibrations for the hydrocarbon chains are given in Figure 2.10 below.

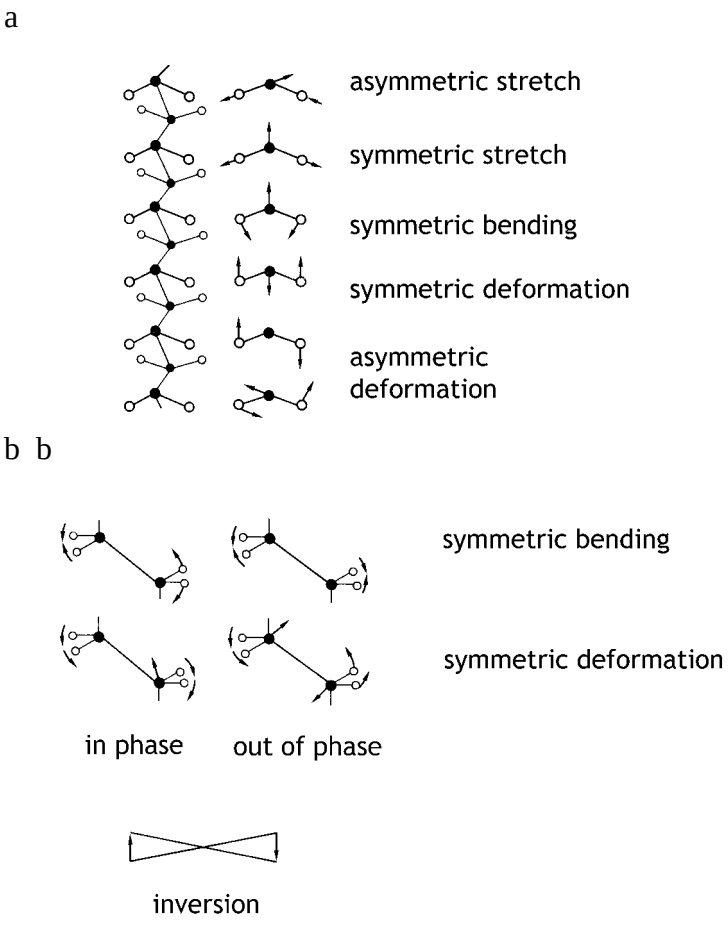

Figure 2.10 Typical vibrations of the hydrocarbon chain of a phospholipid. a, valence and deformation vibrations of methylene groups . b, coupled vibrations between neighboring CH_2-groups

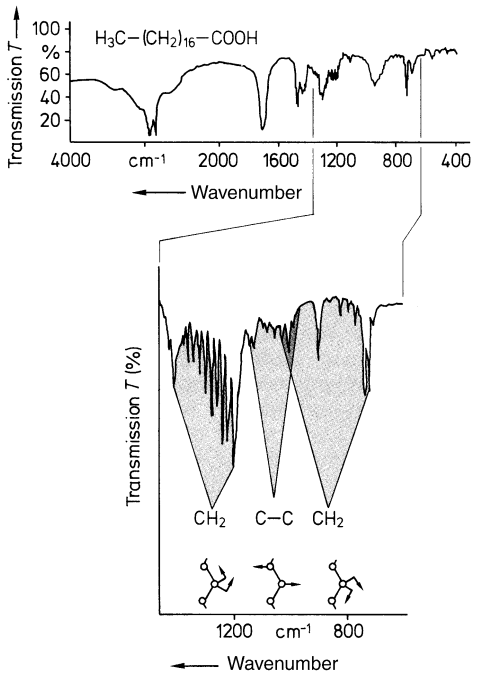

Figure 2.11 IR spectrum of a fatty acid.

2.7. The Michelson Interferometer and Fourier transform techniques.

One of the major disadvantages of the conventional method to produce a spectrum is its inherent slowness. Essentially each point of the spectrum has to be recorded separately - the spectrometer is set to start reading on one end of the spectrum, the frequency is swept smoothly across the whole span of the spectrum, and the detector signal is monitored and digitized or recorded. The inefficiency of such a method is clear when one considers one end to the other in order to find the lines, but most time is spent recording nothing but background noise. Therefore, a different method was developed, Fourier transform spectroscopy, which provides simultaneous and almost instantaneous recording of the whole spectrum in the magnetic resonance, microwave and infrared regions.

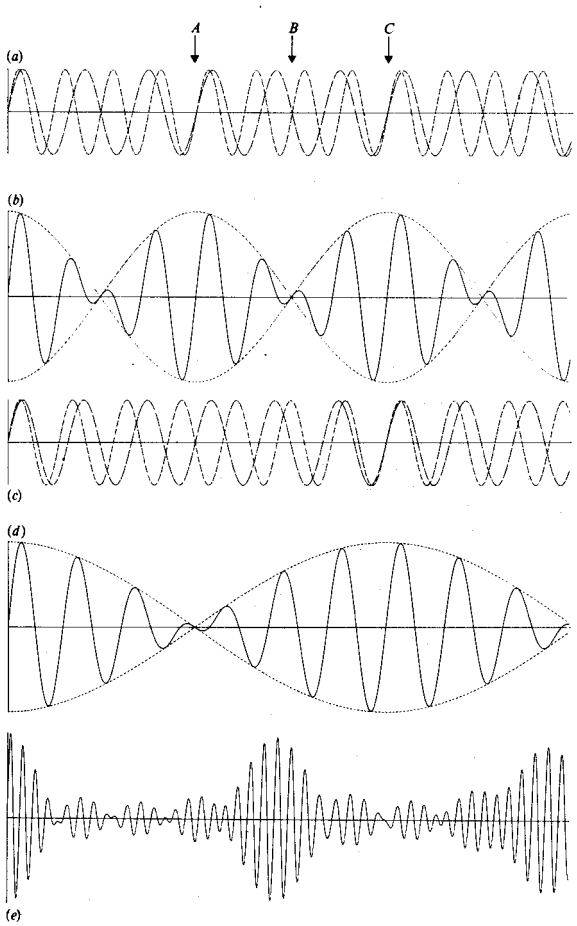

Adding sine waves:
(a) and (c): superposition of two sine waves with slightly different frequencies
(b) and (d): wave that results from the superposition
(e) result of the summation of 5 waves with 5 different frequencies.

(after Banwell: Fundamentals of Molecular Spectroscopy
McGraw-Hill, London, 1983)

Figure 2.12 Superposition of waves of different frequencies

To visualize the principles of fourier transform spectroscopy we take as an example just an emission spectrum of a sample that emits light at a particular frequency. In this example it shall be ignored that the emission band is line broadened and the emitted light shall be of a precise frequency, ν. If the detector is sufficiently fast to respond rapidly to the oscillating signal, its output will be an oscillating signal, again of frequency ν. The detector output is considered a function of time (**time domain spectroscopy** instead of **frequency domain spectroscopy**). Now we consider the sample-emitting radiation at two different frequencies. A detector receiving the total radiation will detect the sum of the two sine waves. The two superimposed waves (for example a and c) and their sum (here b and d) are given in the figure above. The detector output shows an oscillating signal due to the frequencies of the two superimposed waves, but also a periodic change in the amplitude, which slowly increases

and decreases. The periodic change in the amplitude is often called the beat frequency, in analogy to the musical tones that also superimpose. It arises from the two components when they are found “in step”, as in points A and B when the amplitudes reinforce each other and it is also sometimes out of step (as in the point C) where both waves cancel each other. In fact, the beat frequency is always equal to the difference in frequency of the component waves (if they differ in frequency by 10 cycles per second (Hz), then the beat oscillation is also at 10 Hz). This is illustrated by parts (c) and (d) of the figure above, where we show that sine waves with half the frequency separation of those in (a) and (b) and we see that the beat frequency has also halved.

Mathematically it is simple, but tedious, to resolve a combined wave such as those shown above, into its components. Essentially, each component wave has its own frequency and maximum amplitude, so two components require us to evaluate four unknowns from the composite curve. In principle, observation of the time domain signal at four points and solution of four simultaneous equations will yield the required information. Adding more than two sine waves makes the situation even more tedious (see superposition of 5 sine waves with 5 different frequencies). Fortunately, there is quite a simple and general way to resolve a complex wave into its frequency components, the Fourier transform process, named after a french mathematician, Jean Baptiste Fourier, who developed the method in the early 18th century. Even more fortunately, we do not need to know how the method works, as there are modern computers that carry out the transformation.

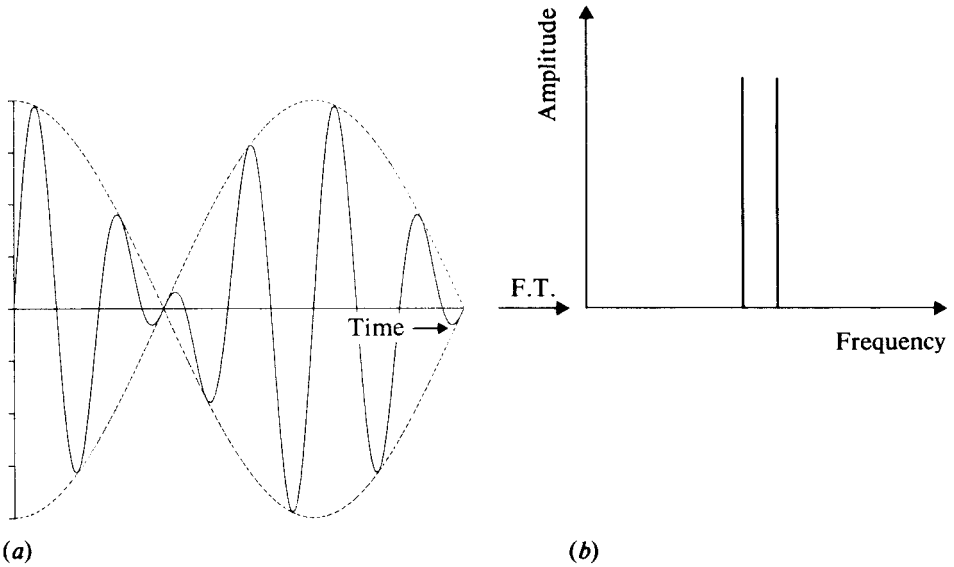

The use of the Fourier transform to convert the summed sine waves of (*a*) into their frequency spectrum, (*b*).

Figure 2.13 Fourier transformation resolves the frequencies of the two waves that compose the detected signal

As an example of its operation we may consider a complex waveform and imagine that a suitable detector is responding to this waveform. A computer receiving the detector output might typically sample it once every millisecond and store about 4000 samplings or more in memory. It will thus need only four seconds to collect the complete signal. The computer would apply the fourier transform process to the stored data in about another second and thus generate the frequency domain spectrum:Essentially the Fourier transform has converted the time domain plot (a) into the frequency domain plot (b) in no more than 5 seconds. Thus, the detector collects all the necessary information simultaneously and the computer decodes this data into the conventional spectrum.

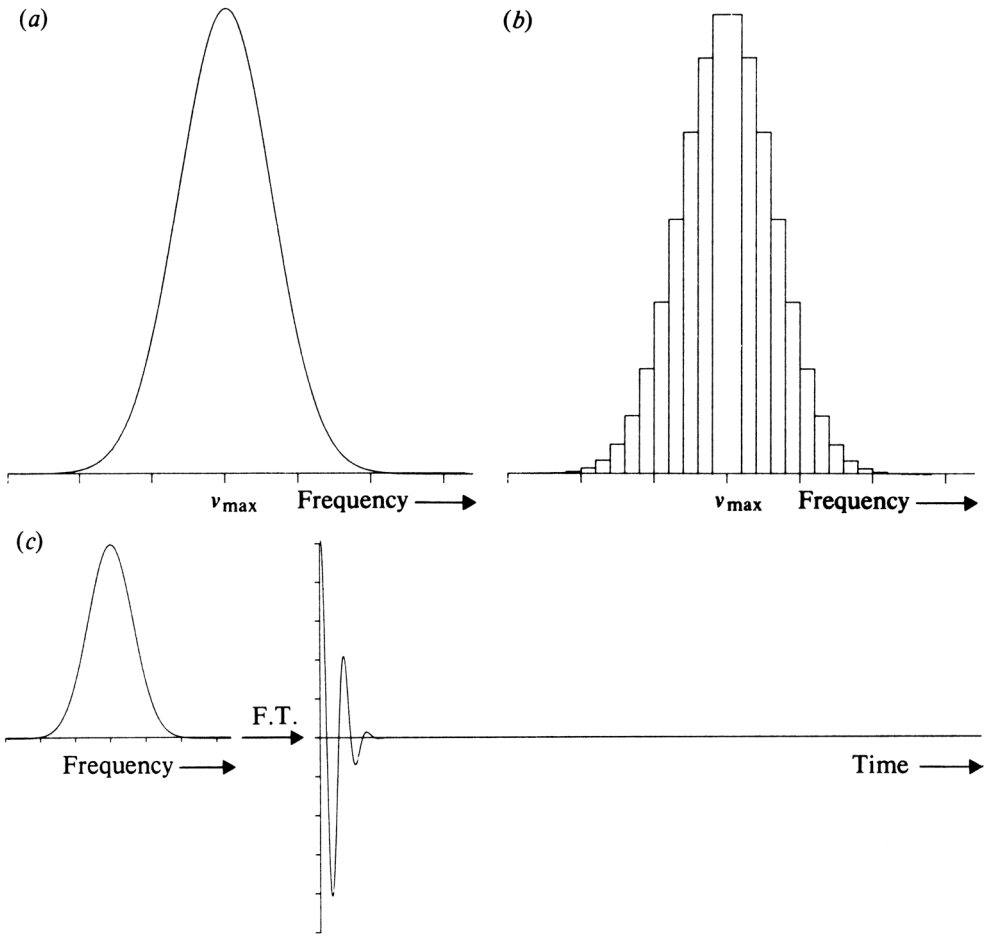

(*a*) shows the frequency distribution of a broad spectral line and (*b*) an approximate histogram of the frequencies; (*c*) is the Fourier transform of (*a*).

Figure 2.14 The time domain signal of a broad spectral line as gernerated by FT.

In this way, FT techniques speed up data collection typically by a factor 10 to 1000. In modern spectroscopy many advances especially in the investigation of biological macromolecules would not be possible without the utility of the Fourier transformation.

When dealing with real samples, we must take into account that real samples do not emit radiation at precise frequencies; as we saw in the previous section, each emission is more or less broadened by various processes, and so each 'line' is really a small package of slightly different frequencies, see the signal of a real gaussian absorption line above. From the histogram that fills the area below the absorption line, it can be deduced that a large number of molecules radiate at the frequency maximum of the radiation package, but that a smaller number of molecules radiates at frequencies away from that maximum, the number decreasing as the separation increases. To detect the total signal emitted by such a package it would be necessary to plot all the sine waves at each frequency using an intensity proportional to the number of molecules radiating at that frequency, and then add all the sine waves together. This is exactly what is done in the reciprocal fourier transform procedure. Just as FT can be used to convert a time domain spectrum into a frequency domain spectrum, the inverse Fourier transformation can be used to convert a frequency domain spectrum into a time domain spectrum. Thus, if the frequency curve of (a) is converted by a computer to the time domain spectrum, the result would be identical to adding the component sine waves (c). We see that a detector receiving the total radiation from a single broad line emission will show an oscillating signal whose overall amplitude decays smoothly to zero. The oscillation is the beat pattern setup by all the superimposed, but slightly different, sine waves in the package to be 'in step' initially, after some time has elapsed, the many different frequencies concerned will be very much out of step, and on average half will have their amplitudes in the positive and half in the negative sense, thus giving a resultant sum of zero.

From a different perspective one can imagine that two waves setting out in step with an infinitesimally small difference in frequency will take an infinite time to get back in step again, i.e. they will never do so. The distribution of frequencies that is present in the absorption band in the figure above, contains many infinitesimally close frequencies. Therefore, none of the individual waves will get back in step again after a few cycles. If the band had been indefinitely broad, i.e., containing an infinite number of infinitesimally close neighbors, none would have ever been in step after the first instant, and the FT of such a white source is a single decaying signal, with no beats.

The corollary of these arguments is that the rate of decay of the overall signal is dependent on the width of the original spectral peak (see figure below):

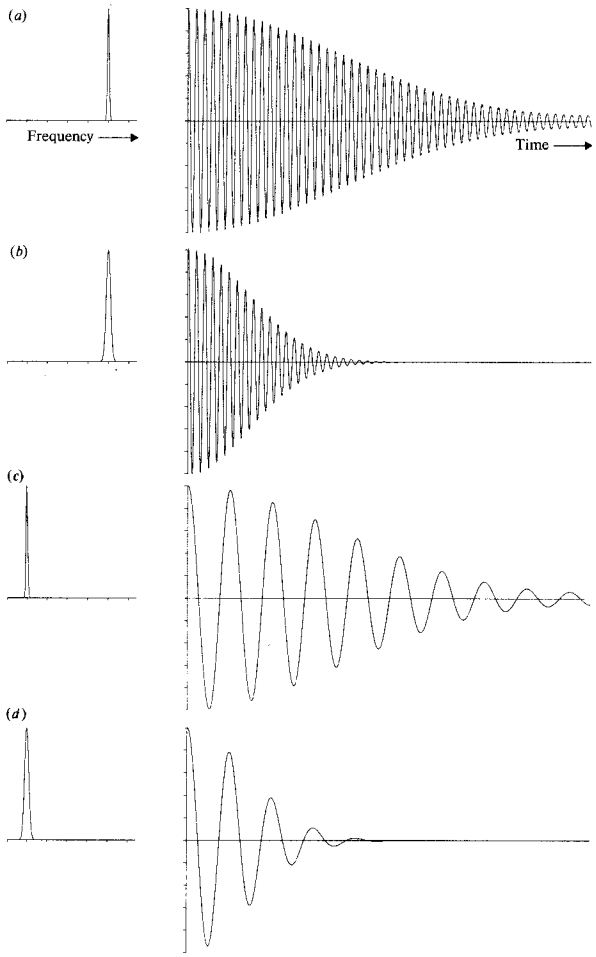

Showing the variation in the time domain signal from a spectral line as its position and breadth vary.

Figure 2.15 Effects of frequency and line width on the time domain spectrum

In (a) it is depicted that the decay of a more narrow signal is slower than the decay of a broader signal at the same central frequency. The beat frequency is identical. On the other hand, Figs. (c) and (d) show the FT of two or more lines with peaks at the same width as in Figure (a) and (b), but at a different central frequency. It can be seen that increasing the frequency of the line gives rise to an increased beat frequency. In general it is clear that the position and width of a frequency package can be recovered from the time domain signal by FT.

Next we must consider that the radiation is composed of more than one frequency, i.e. it has more than one spectral peak. Not surprisingly, the overall result is again summation of the individual peaks (Figure 2.16).

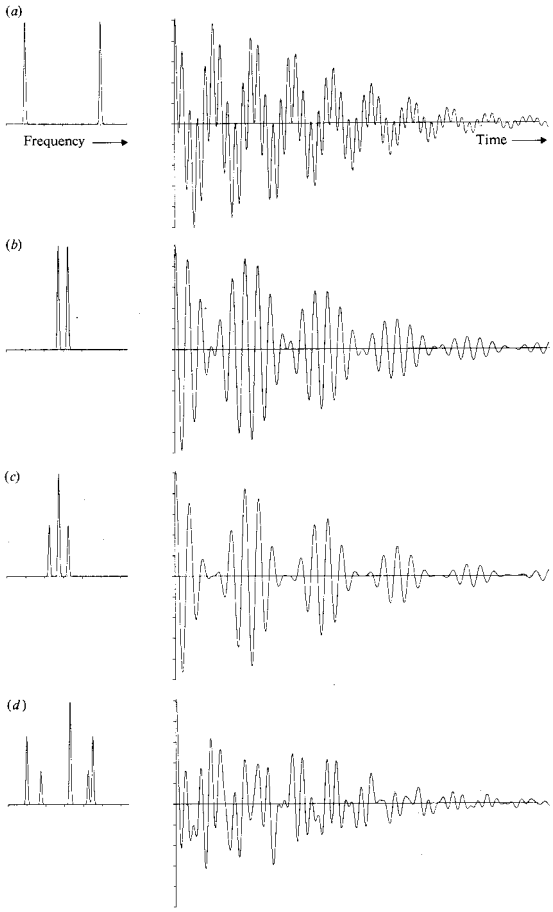

Figure 2.16 Time domain spectra obtained from frequency domain spectra with various bands at different frequencies.

Beat patterns of varying complexity are built up. Figure (a) shows the time domain signal detected from two separate spectral peaks, choosing the frequencies used in the previous figure (a) and (c). In (b) of the figure above, the effect is shown that can be seen in the time domain spectrum when the frequencies are moved closer together. The beat pattern becomes more pronounced if three spectral lines are involved (c) and rather complex, when several randomly space frequency bands of different intensities are emitted, as in (d). The complex patterns of the time domain spectra can be readily transformed into the frequency domain bands by a Fourier transformation.

Finally, we consider the case of an absorption spectrum, to elucidate that the same principles and techniques demonstrated on emission spectra can in principle be applied to absorption spectra as well: As already described above, a “white” source of radiation would show a single decay signal with no beats. An approximation to this is given in the Figure 2.17 (a) below:

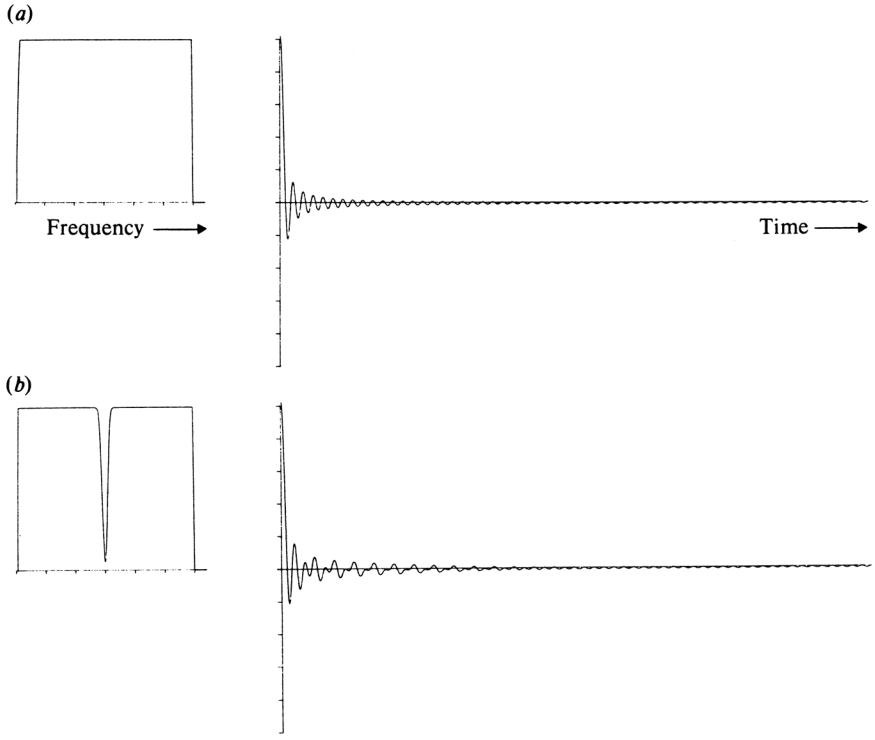

(*a*) An approximation to a 'white' source and its Fourier transform. (*b*) The effect on the Fourier transform of an absorption from the 'white' source.

Figure 2.17 Fourier transform absorption spectroscopy.

Modern spectrometers especially those used in infrared spectroscopy, today almost always make use of Fourier transform techniques to record the spectrum. The heart of the Fourier transform infrared spectrometer is a Michelson interferometer, a device for analyzing the frequencies present in a composite signal.
The total signal from a sample is like a chord, played on a piano and the fourier transform of the signal is equivalent to the separation of the cord into its individual notes, its spectrum.

A Michelson interferometer works by splitting the beam from the sample into two and introducing a varying path difference into one of them. When the two signals are recombined the difference in the path, p, leads to a phase difference between them, and they interfere either constructively or destructively, depending on the difference in path lengths. The detected signal oscillates as the two components alternately come into and out of phase as the path difference is changed. If the radiation has the wavenumber $\tilde{\nu}$, the intensity of the detected signal due to radiation in the range of wavenumbers $\tilde{\nu} = \tilde{\nu} + \Delta\tilde{\nu}$, abbreviated with $I(p,\tilde{\nu})d\nu$,

varies with the difference in path length, p:

$$I(p,\tilde{\nu})d\tilde{\nu} = I(\tilde{\nu})\left(1+\cos\left(2\pi\tilde{\nu}p\right)\right)$$

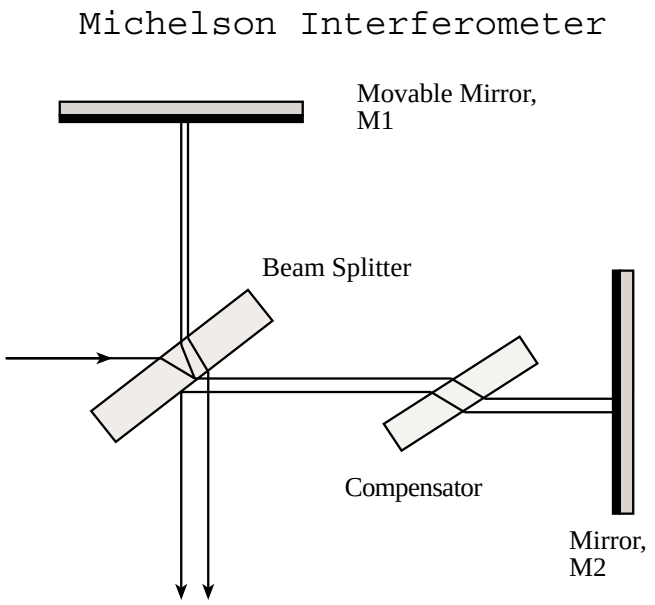

The beam splitting element (a mirror which is transparent for half the insity of the light and which reflects the other half) divides the incident beam into two beams with a path difference that depends on the location of mirror M1.The compensator ensures that both beams pass through the same thickness of material.

When the two beams recombine, they interfere either constructively or destructively depending on the difference in path length.When the path difference is changed, the detected signal oscillates.

Figure 2.18 Michelson Interferometer

Hence, the interferometer converts the presence of a particular wavenumber component in the signal into a variation in intensity of the radiation reaching the detector. An actual signal consists of radiation spanning a large number of wavenumbers, and the total intensity at the detector, abbreviated I(p), is the sum of contributions from all the wavenumbers present in the signal:

$$I(p) = \int_0^\infty I\left(p,\tilde{\nu}\right)d\tilde{\nu} = \int_0^\infty I(\nu)\left(1+\cos\left(2\pi\tilde{\nu}p\right)\right)d\tilde{\nu}$$

The problem is to find $I(\nu)$, the variation of intensity with wavenumber, which is the required spectrum from the record of values of $I(p)$. This step is a standard mathematical technique, the “Fourier transformation” step from which this form of spectroscopy takes its name. Specifically it is:

$$I(\tilde{\nu}) = 4\int_0^{\infty}\left(I(p) - \frac{1}{2}I(0)\right)\left(\cos(2\pi\tilde{\nu}p)\right)dp$$

This integration is usually performed by a computer that is interfaced to the spectrometer, and the output, $I(\tilde{\nu})$, is the absorption spectrum of the sample.

The strong advantage of the Fourier transformation technique is, that all radiation that is emitted by the source is monitored continuously. This is in contrast to a spectrometer in which a monochromator discards most of the radiation. Therefore, Fourier transform spectrometers have a higher sensitivity than conventional spectrometers. The resolution they can achieve is determined by the maximum path length difference, p_{max}, of the interferometer:

$$\Delta\tilde{\nu} = \frac{1}{2p_{\max}}$$

2.8. Special FT-IR techniques

The application of IR spectroscopy to investigate structural elements of biological systems is limited by the presence of water. In biological molecules the interesting resonance frequencies of the C=N, C=O, N-H or O-H vibrations are often hidden by the strong IR absorption of water at around 1600 and 3400 cm^{-1}. Experiments on aqueous systems are therefore possible only with very thin layers and with high concentrations of the molecules of interest. A problem is that the solubility of macromolecules is often small or these macromolecules tend to aggregate. On the other hand, the biological relevance of experiments on dry macromolecules would be questionable.

A way out of this dilemma and a significant improvement of the sensitivity of infrared spectroscopy was achieved with the introduction of the attenuated total internal reflection Fourier transform spectroscopy (see Figure 2.19 below)

Consider a trapezoidal block of a transparent material (germanium, silver chloride, thallium halides). If the chamfer angle is properly chosen, the radiation entering at one end will strike the flat surfaces at less than the critical angle and so will undergo total internal reflection to emerge, only slightly diminished in intensity, at the other end. Although the internal reflection is conveniently called ‘total’, in fact the radiation beam penetrates slightly beyond the surface of the block during each reflection. If sample material is layered to the surface of the block, the beam will travel a small distance through the sample at each reflection (how much depends on the material of which the block is made) and therefore, at when the beam emerges at the end of the block, it will carry the absorption spectrum of the sample - the internal reflection is attenuated, or diminished by sample absorption, hence the name of this type of

.

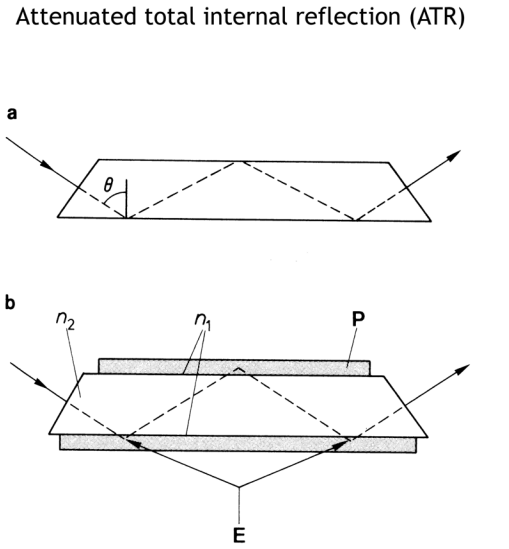

Figure 2.19 Principle of attenuated total internal reflection (ATR) spectroscopy

spectroscopy. The amount of penetration into the sample depends on the wavelength of the radiation and on the of incidence, but is of the order of 10^{-3} to 10^{-4} cm for infrared waves. During its passage through the block, it may undergo some 10-20 reflections, so the total path length through the sample is 10^{-3} to 10^{-2} cm, which is a short, but often perfectly adequate, path length for the production of a reasonable spectrum.

The block must be of a material that is infrared transparent and must have a refractive index higher than that of the sample, otherwise internal reflection will not occur. The block is typically 5 cm long, 2 cm wide, and 0.5 cm thick. The sample material can be liquid or solid but not gaseous (the path length of 10^{-2} cm would be much to short in this case), provided it can be kept in close contact with the block. The technique is usually reserved to study samples that are difficult to study by ordinary means. Thus it is virtually impossible to study fibrous material by transmission — the rough surface scatters all the radiation falling on it; but if the fibres are clamped firmly to the outside of the block, quite acceptable spectra result.

2.8.1 Examples for the use of ATR-FTIR-spectroscopy.

ATR-FTIR spectroscopy is often used in the investigation of membrane proteins (which account to about 50%) of all proteins. To investigate membrane proteins in ATR-FTIR experiments, the protein must be placed on a block of IR-transparent material in its native environment, a phospholipid bilayer (insert transparency showing the lipid bilayer). This can

be accomplished by using the Langmuir/Blodgett/Schaefer technique for the generation of the so-called supported phospholipid bilayers (Figure 2.20). A lipid mono-layer is first transferred from the air-water interface of a Langmuir trough to the hydrophilic support at a constant surface pressure of 32-36 mN/m, i.e. the bilayer equivalence pressure. A second monolayer is deposited onto this surface by horizontal apposition of the substrate to a monolayer at the same pressure. The substrate with the bilayer is then collected in a dish or measuring cell under water, avoiding any subsequent exposure to air. Fully hydrated high quality bilayers are obtained in this way. However, this method is inadequate for reconstituting membranes proteins. A second method to prepare supported bilayers is by spreading vesicles on a hydrophilic substrate. A dispersion of small unilamellar lipid vesicles, which may also include reconstituted

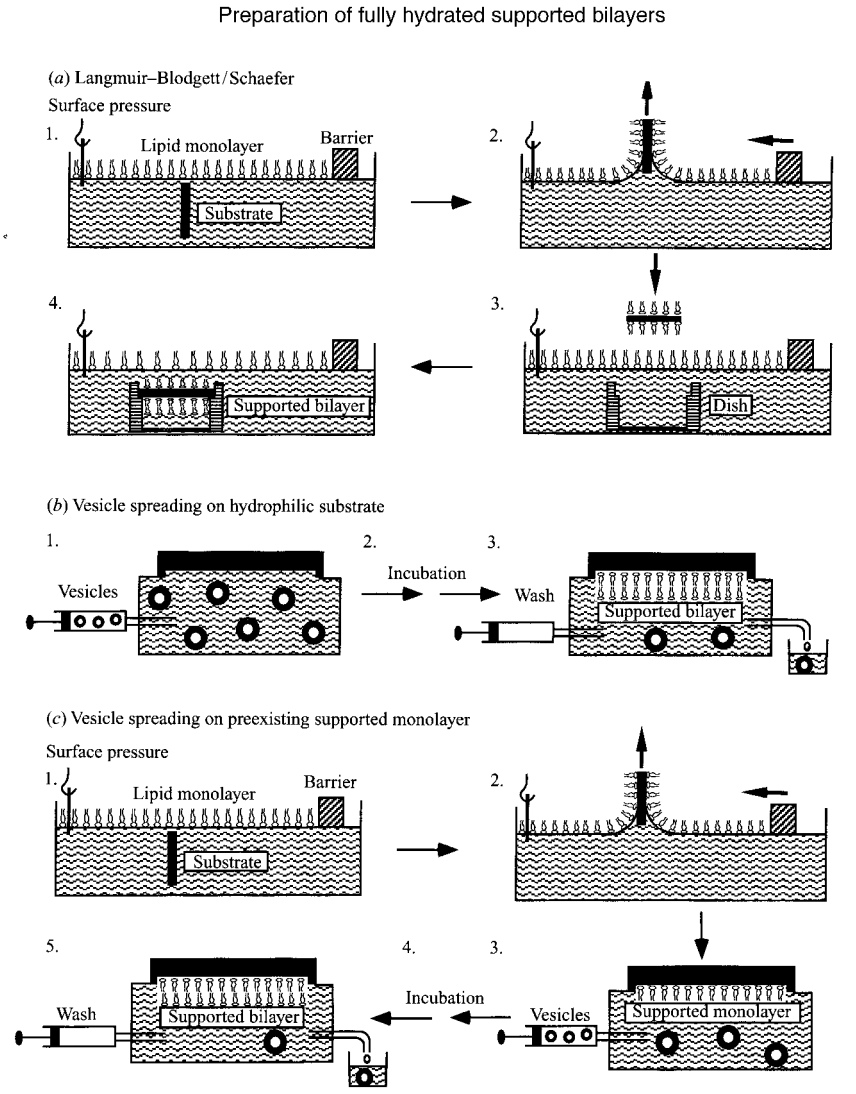

Methods for preparation of fully hydrated supported lipid bilayers. (*a*) Langmuir-Blodgett/Schaefer technique. (*b*) Spreading of small unilamellar vesicles on a hydrophilic substrate. (*c*) Spreading of small unilamellar vesicles on a preexisting supported monolayer.

Figure 2.20 Techniques to prepare supported bilayers for the use in ATR spectroscopy.

membrane proteins is brought into contact with the clean surface of the internal reflection

element assembled in a liquid holding cell. These vesicles will spontaneously spread on the substrate and form a continuous planar bilayer in about an hour at room temperature. Again, these bilayers must not be exposed to air after formation, but excess vesicles can be easily flushed out of the cell by a large volume of buffer. Most of the studies performed today have been performed with third method, in which vesicles are spread on a preexisting monolayer. In this method, which is also often referred to as monolayer fusion, a lipid mono-layer is first transferred from the air-water interface of a Langmuir trough to the hydrophilic internal reflection element at the bilayer equivalence pressure. The monolayer-coated plate is then assembled in the ATR holding cell and a dispersion of lipid vesicles with or without protein is then injected. As in the direct spreading method, a bilayer forms by spontaneous self-assembly and excess vesicles are removed by flushing the cell with buffer. A D_2O containing buffer may be introduced either at this or at a later stage. This monolayer fusion method allows the reconstitution of integral membrane proteins.

Samples like the supported bilayers on a total internal reflection element are different from samples that are prepared in normal cuvette. In a cuvette, the samples are isotropically oriented an the radiation interacts with the molecules from any possible direction. By contrast, on a supported bilayer the samples are oriented an additional information can be obtained.

As an example we consider the UV-absorption spectrum of Poly-L-glutamine. The absorption of the UV light is monitored parallel and perpendicular to the long axis of the molecules. The absorption is different, because changes in the transition dipole moment of the molecules have different components along the two axis. The different absorption in the two directions is called *Linear Dichroism*. For each substance there is a specific ratio of the extinction coefficients

$$d = \frac{\varepsilon_{||} - \varepsilon_{\perp}}{\varepsilon_{||} + \varepsilon_{\perp}}$$

with the Beer Lambert Law

$$A = \log\left(\frac{I_0}{I}\right) = -\log(T) = \varepsilon \cdot c_M \cdot l$$

the dichroic ratio is also given as

$$d = \frac{A_{||} - A_{\perp}}{A_{||} + A_{\perp}}$$

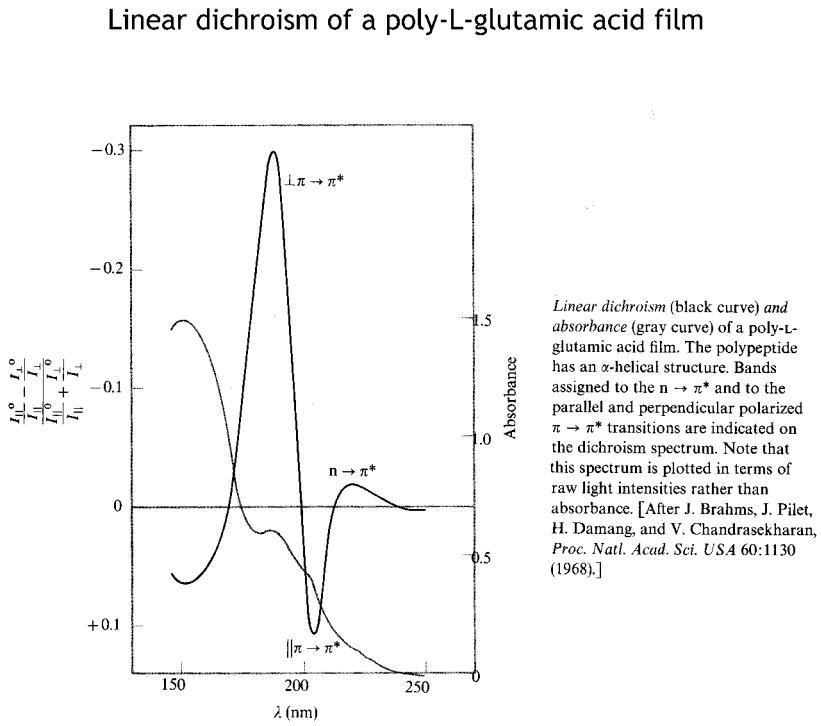

Linear dichroism (black curve) *and absorbance* (gray curve) of a poly-L-glutamic acid film. The polypeptide has an α-helical structure. Bands assigned to the $n \rightarrow \pi^*$ and to the parallel and perpendicular polarized $\pi \rightarrow \pi^*$ transitions are indicated on the dichroism spectrum. Note that this spectrum is plotted in terms of raw light intensities rather than absorbance. [After J. Brahms, J. Pilet, H. Damang, and V. Chandrasekharan, *Proc. Natl. Acad. Sci. USA* 60:1130 (1968).]

Figure 2.21 Linear dichroism of poly-L-glutamic acid

To determine the dichroic ratio, it is necessary to use linearly polarized light (i.e. the electrical field vector of the light oscillates only in one direction). If the transition dipole moment is known for a particular absorbance, one can determine the direction of the molecule by measuring the dichroic ratio.

Linear dichroism of lipid molecules in supported planar bilayers
by ATR-FTIR spectroscopy

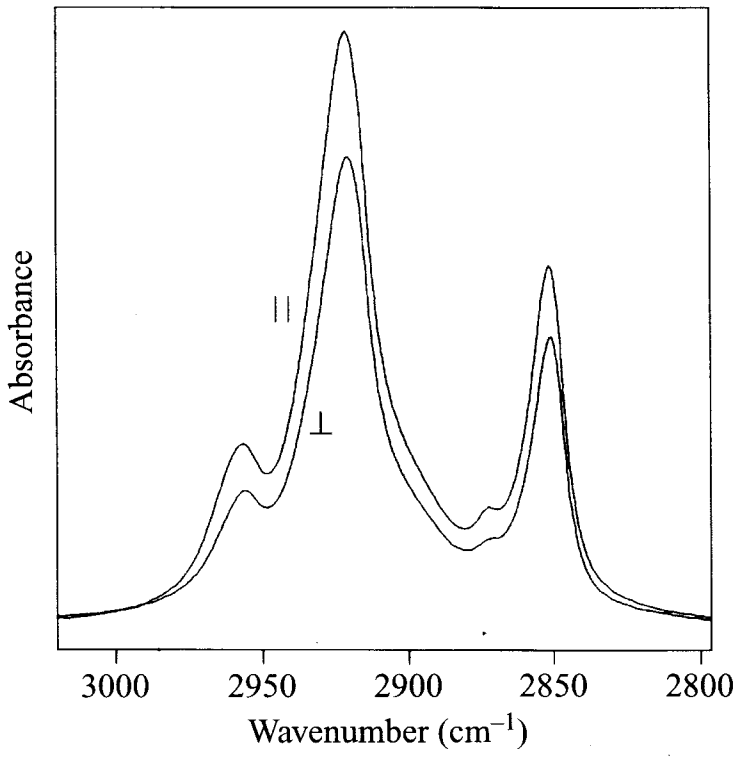

ATR–FTIR spectra in the methylene stretching region of a fully hydrated single supported bilayer of DMPC, prepared by the monolayer fusion technique, at parallel and perpendicular polarizations of the IR beam. The measuring temperature was approximately 21 °C. The dichroic ratio and the derived order parameter are 1·25 ± 0·02 and 0·45 ± 0·02, respectively. (Reproduced from Tatulian *et al.* 1995*b*.)

Figure 2.22 Linear dichroism of phospholipid molecules obtained by ATR-FTIR spectroscopy.

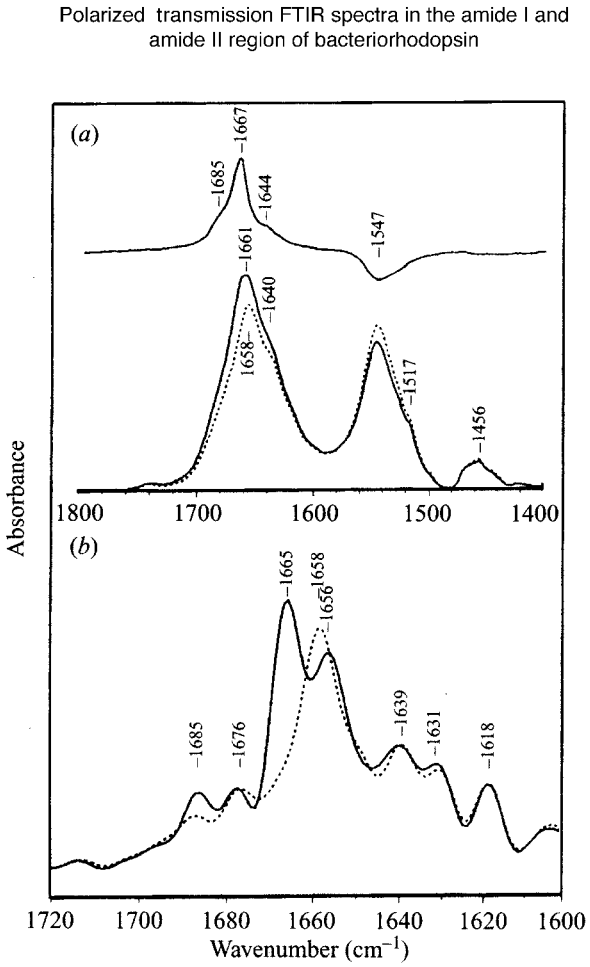

Polarized transmission FTIR spectra in the amide I and II region of bacteriorhodopsin in hydrated oriented purple membranes. (*a*) Spectra recorded with a parallel (solid line) and perpendicular (dashed line) polarized IR beam. The spectrum on the top is the linear dichroism spectrum, $A_{\parallel}-A_{\perp}$. (*b*) Expanded amide I region of spectra recorded with a parallel (solid line) and perpendicular (dashed line) polarized IR beam at 80 K after Fourier self-deconvolution. The main amide I peak is split into two components ($\sim$ 1665 and $\sim$ 1656 cm^{-1}) of which the higher frequency component exhibits stronger dichroism.

Figure 2.23 Polarized FTIR spectra of bacteriorhodopsin in the amide I and amide II regions.

1928 *Biochemistry, Vol. 34, No. 6, 1995*

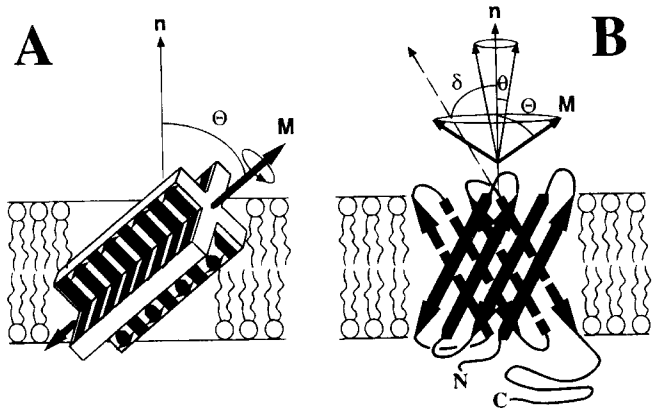

FIGURE 8: Models illustrating symmetry relations between β-sheets, their amide I transition dipole moments, and a planar lipid bilayer. *Panel A:* The orientation of planar antiparallel β-sheets is not uniquely determined by the angle Θ between the transition dipole moment M and the membrane normal n. The β-sheets can assume many orientations that are rotationally symmetric around M. Two orthogonal orientations are shown. When $\Theta = 0°$, the strands run parallel to the plane of the membrane, but adjacent strands of the sheet penetrate the membrane. When $\Theta = 90°$, the strands may run parallel to the plane of the membrane with alternating residues up and down, respectively, or they may be oriented parallel to the membrane normal. *Panel B:* The orientation of a β-barrel relative to the bilayer normal (angle θ) is determined by the angle Θ and the angle δ of the strands relative to the bilayer normal.

Figure 2.24

2.9. Approximate frequencies of amino acid side chain absorptions in the 1400-1800 cm^{-1}-region.

Vibration			in H_2O ν_0 (cm^{-1})	in D_2O ν_0 (cm^{-1})
Phe	ring		1494	
Tyr	ring—0^-		1498	1500
terminal	—NH^{3+}	(δ_s)	1515	
Tyr	ring-OH		1518	1615,1515
Lys	—NH^{3+}	(δ_s)	1526	
terminal	-NH_2	(δ)	1560	
Glu	—COO^-	(ν_{as})	1560	1567
Asp	—COO^-	(ν_{as})	1574	1584
His	ring		1596	
terminal	—COO^-	(ν_{as})	1598	1592
Tyr	ring--0-		1602	1603
Gln	—NH_2	(δ)	1610	
Asn	—NH_2	(δ)	1622	
Lys	—NH^{3+}	(δ_{as})	1629	
terminal	—NH^{3+}	(δ_{as})	1631	
Arg	—$CN_3H_5^+$	(ν_s)	1633	1586
Gln	—C=O	(ν)	1670	1635
Arg	—$CN_3H_5^+$	(ν_{as})	1673	1608
Asn	—C=O	(ν)	1678	1648
Glu	—COOH	(ν)	1712	1706
Asp	—COOH	(ν)	1716	1713
terminal	—COOH	(ν)	1740	1720

'Adapted from Chirgadze et al., 1975 and Venyaminov & Kalnin, 1990a,b

δ_s: symmetric deformation vibration (bending vibration)
δ_{as}: asymmetric deformation vibration
ν_s: symmetric stretching vibration
ν_{as}: asymmetric stretching vibration

Table 2.3 IR absorption frequencies of amino acid sidechains.

In nucleic acids the melting of the double helix can be monitored by IR spectroscopy.

2.10. Fine Structure of Infrared Spectra

Rotational spectra and the rotating diatomic molecule.

Rotational energy, like other forms of molecular energy is quantized, which means that a molecule cannot have any arbitrary amount of rotational energy (and thus an arbitrary value of its angular momentum). The energy is limited to certain definite values, depending on the shape and the size of the molecule concerned. The permitted energy values — the so-called rotational energy levels — can in principle be calculated by the Schrödinger equation. But even for simple molecules the mathematical analysis is complex and for bigger molecules, it is necessary to work with approximations. Here we will just describe some very basic principles on the example of a simple diatomic molecule.

The rigid diatomic molecule

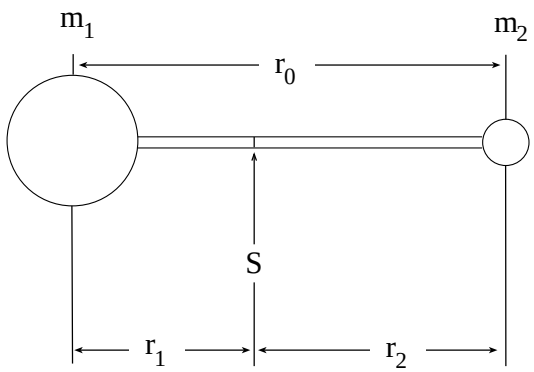

A rigid diatomic molecule treated as two masses connected at a rigid distance. S: center of gravity.

Figure 2.25 The rigid diatomic molecule

Two atoms (or masses) are joined by a rigid bar (the bond) whose length is

$$r_0 = r_1 + r_2$$

The molecule rotates end-over-end about a point S, the center of gravity, which is defined by the moment of balancing equation:

$$m_1 r_1 = m_2 r_2$$

The moment of inertia about C is defined by:

$$I = m_1 r_1^2 + m_2 r_2^2$$

or

$$I = m_2 r_2 r_1 + m_1 r_1 r_2 = r_1 r_2 (m_1 + m_2)$$

Since $m_1 r_1 = m_2 r_2 = m_2 (r_0 - r_1)$ the distances r_1 and r_2 from the center of gravity can be substituted by the distance r_0 between the two atoms (masses):

$$r_1 = \frac{m_2 r_0}{m_1 + m_2} \text{ and } r_2 = \frac{m_1 r_0}{m_1 + m_2}$$

The moment of inertia can now be written as

$$I = \frac{m_1 \cdot m_2}{m_1 + m_2} r_0^2 = \mu r_0^2$$

The quotient

$$\mu = \frac{m_1 \cdot m_2}{m_1 + m_2}$$

is called the reduced mass of the system. The moment of inertia for the diatomic molecule is therefore described by the atomic masses and the bond length.

Applying the Schroedinger equation to the rotating diatomic molecule, it can be shown that the rotational energy levels are given by the expression:

$$E_j = \frac{h^2}{8\pi^2 I} \cdot J \cdot (J+1), \text{ with J = 0, 1, 2, 3, ...}$$

I is the moment of inertia, h is Planck's constant, and J is the rotational quantum number. As a direct result of solving the Schroedinger equation, J can only be zero or a positive integer number. Therefore the rotational energy can have only discrete values, the energy levels of rotation of the molecule. The corresponding frequencies, $\nu = \frac{\Delta E}{h}$, or wavenumbers of rotation,

$\tilde{\nu} = \frac{\Delta E}{hc}$ can also be used to define the possible energy levels. For rotational and vibrational spectroscopy it is common to describe the energy levels in wavenumbers (cm^{-1}):

$$\varepsilon_j = \frac{E_J}{hc} = \frac{h}{8\pi^2 Ic} J(J+1) \qquad (cm^{-1})$$

The equation is usually simply written as:

$$\varepsilon_J = BJ(J+1) \qquad (cm^{-1}) \qquad \text{with} \quad B = \frac{h}{8\pi^2 I_B c} \qquad (cm^{-1})$$

The relation between the rotational quantum number J and the energy levels ε_j allow us to draw the energy diagram. For J=0 the energy is also 0 and the molecule does not rotate. For J=1 the energy is 2B and the molecule has its lowest angular momentum. These and higher energy levels are given in Figure 2.26 below:

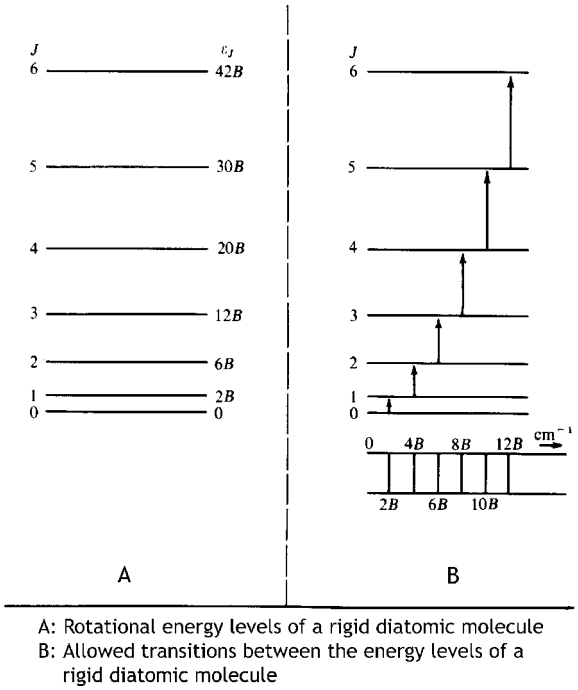

Figure 2.26 Rotational energy levels of the rigid diatomic molecule

In principle, there is no limit how rapidly a molecule may rotate. However, the centrifugal force on the atoms may be greater then the strength of the bond and the molecule is then disrupted, but this point is not reached at normal temperatures.

As indicated in the Figure above, the energy difference between different rotational states depends on the levels between a transition takes place. If we imagine the molecule to be in

the ground state (J=0) the incident radiation can be absorbed to raise it to the J=1 state. The energy that is necessary is given by

$$\varepsilon_{J=1} - \varepsilon_{J=0} = 2B - 0 = 2B \ [\text{cm}^{-1}]$$

In other words, an absorption line will appear at 2B cm^{-1}.

If the molecule is then raised from the J=1 to the J=2 level by absorption of more energy, the corresponding energy difference is

$$\tilde{\nu}_{J=1\to J=2} = \varepsilon_{J=2} - \varepsilon_{J=1}$$
$$= 6\ \text{B} - 2\ \text{B} = 4\ \text{B}\ (\text{cm}^{-1})$$

In general to raise the molecule from the state J to state J+1, we would have:

$$\begin{aligned}\tilde{\nu}_{J\to J+1} &= B(J+1)(J+2) - BJ(J+1)\\ &= B(J^2 + 3J + 2 - J^2 - J)\\ &= B(2J+2)\\ &= 2B(J+1)\end{aligned}$$

Thus, a incremental raise of the energy of rotation leads to absorption lines at 2B, 4 B, 6B, 8B, ..., cm^{-1}. Until now, we have assumed that transitions between energy levels occur only between immediate neighbors on the energy scale. We have not considered that transitions may occur, for example between J=0 and J =2. Quantum mechanical consideration show that such transitions are indeed “forbidden”. The selection rule for transitions between rotational energy levels is $\Delta J = \pm 1$.

The relation

$$\tilde{\nu}_{J\to J+1} = 2B(J+1)$$

gives the *whole* spectrum of the molecule, provided that the molecule has a dipole moment (it has to be asymmetric, heteronuclear). HCl, NO, CO will show a rotational spectrum, while H_2, CO_2, N_2 and O_2 will not.

2.10.1 Effect of isotopic substitution.

When one atom in the molecule is replaced by its isotope, the same element but with a different number of neutrons in the nucleus and therefore with a different mass, the resulting molecule is chemically identical with the original molecule. In particular, there is no appreciable

change in internuclear distance on isotopic substitution. However, there is a change in the reduced mass of the molecule, which results in change of the moment of inertia

$$I = \frac{m_1 \cdot m_2}{m_1 + m_2} r_0^2 = \mu r_0^2 .$$

The moment of inertia is directly related to the rotational constant B

$$B = \frac{h}{8\pi^2 I_B c}$$

Gilliam et al. found the first rotational absorption line of $^{12}C^{16}O$ to be at 3. 84235 cm^{-1}, while that of $^{13}C^{16}O$ was at 3.67337 cm^{-1}. The values of B can be calculated from these wavenumbers: B($^{12}C^{16}O$)=1.92118 cm^{-1}, B($^{13}C^{16}O$)=1.83669 cm^{-1}. The ratio B($^{12}C^{16}O$) / B($^{13}C^{16}O$) is then:

$$\frac{\mathrm{B}(^{12}\mathrm{C}^{16}\mathrm{O})}{\mathrm{B}(^{13}\mathrm{C}^{16}\mathrm{O})} = \frac{h}{8\pi^2 I(^{12}\mathrm{C}^{16}\mathrm{O})c} \cdot \frac{8\pi^2 I(^{13}\mathrm{C}^{16}\mathrm{O})c}{h} = \frac{I(^{13}\mathrm{C}^{16}\mathrm{O})}{I(^{12}\mathrm{C}^{16}\mathrm{O})}$$

and finally

$$\frac{\mathrm{B}(^{12}\mathrm{C}^{16}\mathrm{O})}{\mathrm{B}(^{13}\mathrm{C}^{16}\mathrm{O})} = \frac{\mu(^{13}\mathrm{C}^{16}\mathrm{O})}{\mu(^{12}\mathrm{C}^{16}\mathrm{O})}$$

which is 1.046. The introduction of the isotope ^{13}C into carbon monoxide thus leads to smaller wavenumbers of the absorbed radiation (and therefore longer wavelength and smaller frequencies).
The composition of isotopes in a given substance can be determined using rotational absorption spectroscopy.

Until now, it was assumed that the bond is rigid. However, we know that there are vibrations between the connected atoms. These vibrations result in a change of the distance between the atoms. Furthermore, increased rotational energy and an increase in the rotational frequency results in an increase of the centrifugal force that works against the force that connects the two atoms. Thus, the bond length will increase with the rotational frequency.

$$F = -k(r - r_0) = 4\pi^2 \nu_{rot}^2 r\mu$$
$$r = \frac{kr_0}{\left(k - 4\pi^2 \nu_{rot}^2 \mu\right)}$$

From vibrational spectroscopy we know that in case of a harmonic oscillation, the oscillation frequency is given by

$$\nu_{vib} = \frac{1}{2\pi}\sqrt{\frac{k}{\mu}}$$

which can be rearranged to give the force constant k:

$$k = 4\pi^2\nu_{vib}^2\mu = 4\pi^2\tilde{\nu}_{vib}^2 c^2\mu$$

where $\tilde{\nu}$ is the wavenumber (in cm^{-1}), c the speed of light, μ the reduced mass and k the force constant of the vibration.

The second consequence of elasticity is that the quantities B and r vary during a vibration.

From the definition of B

$$B = \frac{h}{8\pi^2 I_B c} = \frac{h}{8\pi^2 c\mu r^2}$$

it follows that B is proportional to the reciprocal square of the distance between the two atoms. However, in a simple harmonic motion a molecular bond is compressed and extended an equal amount on each side of the equilibrium distance (r_e). The average value of this distance is therefore unchanged. The average value of $1/r^2$ is not equal to the average value of $1/r_e^2$. To give an example, we consider a bond of an equilibrium length, 0.1 nm that vibrates between the limits 0.09 and 0.11 nm. We have:

$$\langle r\rangle_{av} = \frac{0.09 + 0.11}{2} = 0.1 = r_e$$

and

$$\left\langle \frac{1}{r^2}\right\rangle_{av} = \frac{\left(1/0.09\right)^2 + \left(1/0.11\right)^2}{2} = 103.05\ \text{nm}^2$$

which results in a radius of $\sqrt{103.05\ \text{nm}^2} = 0.0985\ \text{nm}$. The difference is not negligible compared with the precision with which B can be measured spectroscopically.
The mathematical treatment of the non-rigid rotator in quantum mechanics gives the rotational energy levels as

$$E_J = \frac{h^2}{8\pi^2 I} J(J+1) - \frac{h^4}{32\pi^4 I^2 r^2 kc} J^2(\mathrm{J}+1)^2 \quad (\text{in cm}^{-1})$$

or

$$\varepsilon_J = \frac{E_J}{hc} = BJ(J+1) - DJ^2(J+1)^2 \qquad (\text{in cm}^{-1})$$

A comparison of the energy levels of a rigid and non-rigid rotator is given in Figure 2.27 below.

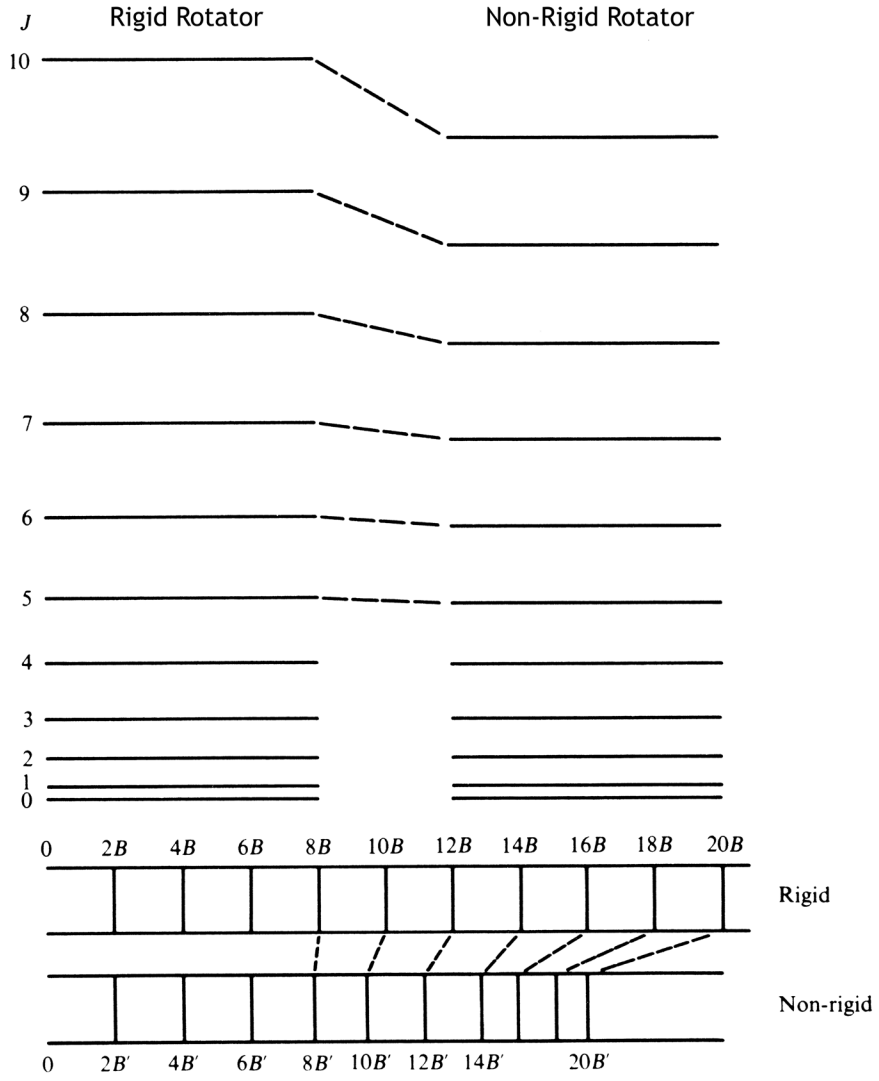

Figure 2.27 Energy levels of the rigid and non-rigid rotator

A typical diatomic molecule has rotational energy separations of 1-10 cm^{-1}. In contrast we saw that vibrational transitions have energy separations in the region of 400 to 4000 cm^{-1}. Since the energy levels are separated by very different margins, we may in approximation consider that a diatomic molecule can execute rotations and vibrations independently of each other. This assumption is called the Born-Oppenheimer approximation (although this includes the separation of different energy levels of electrons in electron transitions).

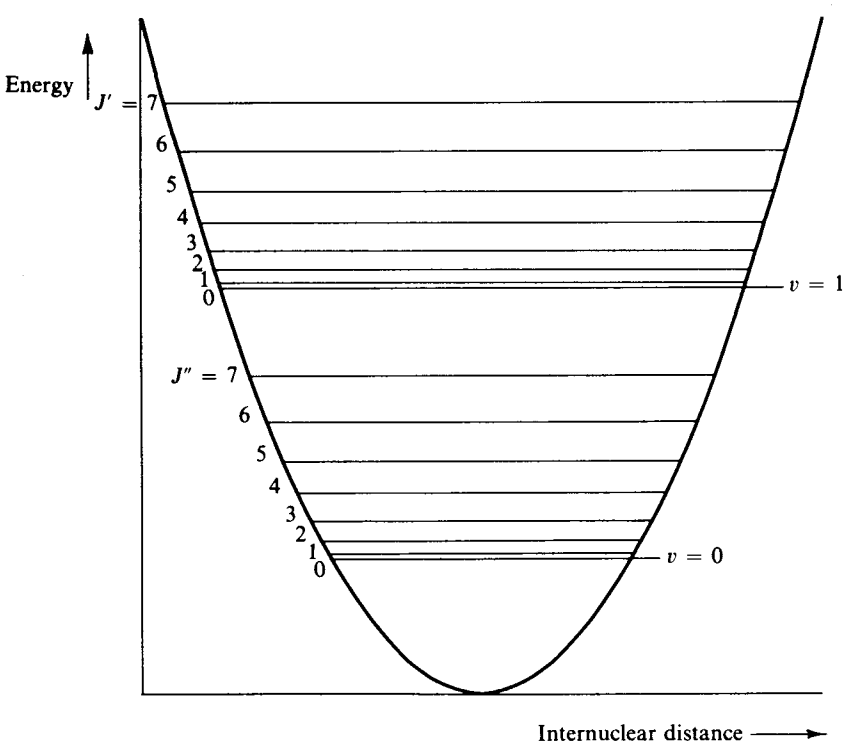

The rotational energy levels for two different vibrational states of a diatomic molecule.

Figure 2.28 Rotational energy levels of two vibrational modes.

This approximation includes that the energy of a given system is simply the sum of the separate energies:

$$E_{total} = E_{rot} + E_{vib}$$

in Joule, or

$$\varepsilon_{total} = \varepsilon_{vib} + \varepsilon_{rot}$$

Taking the separate expressions for ε_{vib} and ε_{rot} the total energy is given by:

$$\varepsilon_J = BJ(J+1) - DJ^2(J+1)^2 + HJ^3(J+1)^3$$
$$+\left(v+\frac{1}{2}\right)c\tilde{\nu}_{vib} - x\left(v+\frac{1}{2}\right)^2 c\tilde{\nu}_{vib}$$

If the centrifugal distortion constants are neglected the equation can be written:

$$\varepsilon_{total} = \varepsilon_{j,v} = BJ(J+1) + \left(v+\frac{1}{2}\right)c\tilde{\nu}_{vib} - x\left(v+\frac{1}{2}\right)^2 c\tilde{\nu}_{vib}$$

(It should be noted that it is not logical to ignore D, since the molecule is treated as vibrating, but not rigid. However if D is taken into account, the effect on the spectrum would still be minor because of the large separation in the energy levels of a vibration compared to a rotation).

In the figure above (previous page), the energy levels for rotation and vibration are sketched for the lowest levels of vibration, v=0 and v=1. The relative proportions of energy differences in vibration and rotation are neglected in this graph, since separations in rotational energy levels are only 1/1000 of the separations of vibrational energy levels.

Since the rotational constant B is assumed to be unaffected by differences in the values of J and v (a consequence of the Born-Oppenheimer Approximation), the separations between the rotational energy levels at the vibrational level v=0 is the same as that of the rotational energy levels at the vibrational level v=1.

The selection rules for the combined motions are the same as the selection rules for each separately:

$$\Delta v = 0,\ \pm 1,\ \pm 2,\ \pm 3\ \ldots.\ ;\quad \Delta J = \pm 1$$

The case Δv=0 is the simple case of a transition between rotational energies only. Quantum mechanical considerations show that a diatomic molecule, with very rare and special exceptions must not undergo vibrational transitions with no change in the rotational energy (ΔJ must not be 0).

The vibration-rotation spectrum for the transition from v=0 to v=1 can be obtained with the

selection rules:

$$\Delta\varepsilon_{v,J} = \varepsilon_{J',v=1} - \varepsilon_{J'',v=0}$$

$$\begin{aligned}\Delta\varepsilon_{v,J} &= BJ'(J'+1) + 1\frac{1}{2}\tilde{\nu}_e - 2\frac{1}{4}x_e\tilde{\nu}_e - \left\{BJ''(J''+1) + \frac{1}{2}\tilde{\nu}_e - \frac{1}{4}x_e\tilde{\nu}_e\right\} \\ &= \tilde{\nu}_0 + B(J'-J'')(J'+J''+1) \quad (\text{in cm}^{-1}), \qquad \text{with } \tilde{\nu}_0 = \tilde{\nu}_e(1-2x_e)\end{aligned}$$

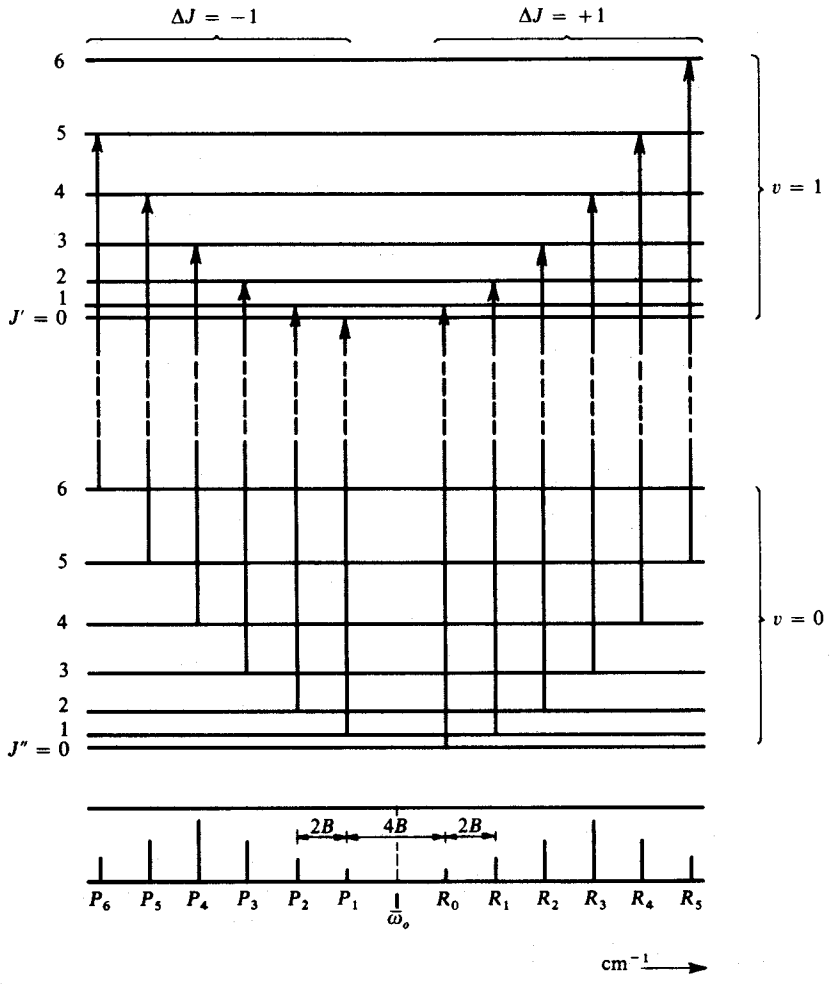

Some transitions between rotational-vibrational energy levels of a diatomic molecule together with a spectrum arising from these transitions.

Figure 2.29 Transitions between two vibrational modes and rotational fine structure.

B is taken identical in the upper and lower vibrational states, which is a direct consequence of the Born-Oppenheimer approximation – rotation is unaffected by vibrational changes.

If we have:

1. $\Delta J = +1,\ i.e.\ J' = J'' + 1 \quad \text{or} \quad J' - J'' = +1$

the energy difference is

$$\Delta\varepsilon_{v,J} = \tilde{\nu}_0 + 2B(J''+1) \quad \text{cm}^{-1}, \qquad J'' = 0,1,2.....$$

If we have:

2. $\Delta J = -1,\ i.e.\ J'' = J' + 1 \quad \text{or} \quad J' - J'' = -1$

the energy difference is

$$\Delta\varepsilon_{v,J} = \tilde{\nu}_0 - 2B(J'+1) \quad \text{cm}^{-1}, \qquad J' = 0,1,2.....$$

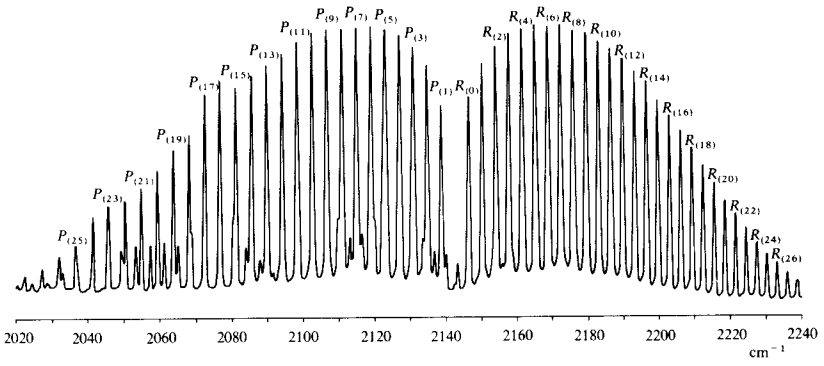

Rotation-vibration spectrum of carbon monoxide (at a gas pressure of 120 mbar). The lines are labeled according to their J values. The P-branch is complicated by the presence of a band centered at about 2100 cm^{-1} due to one per cent of ^{13}CO in the sample; Some of the rotational lines from this band appear between P branch lines, others are overlapped by a P-branch line and give it an enhanced intensity.

Figure 2.30 Rotational vibrational spectrum of carbon monoxide.

In combination it can be written:

$$\Delta\varepsilon_{v,J} = \tilde{\nu}_0 + 2Bm \quad (\mathrm{cm}^{-1}), \qquad m = \pm 1, \pm 2.....$$

The last equation represents the combined rotation-vibration spectrum. It will consist of

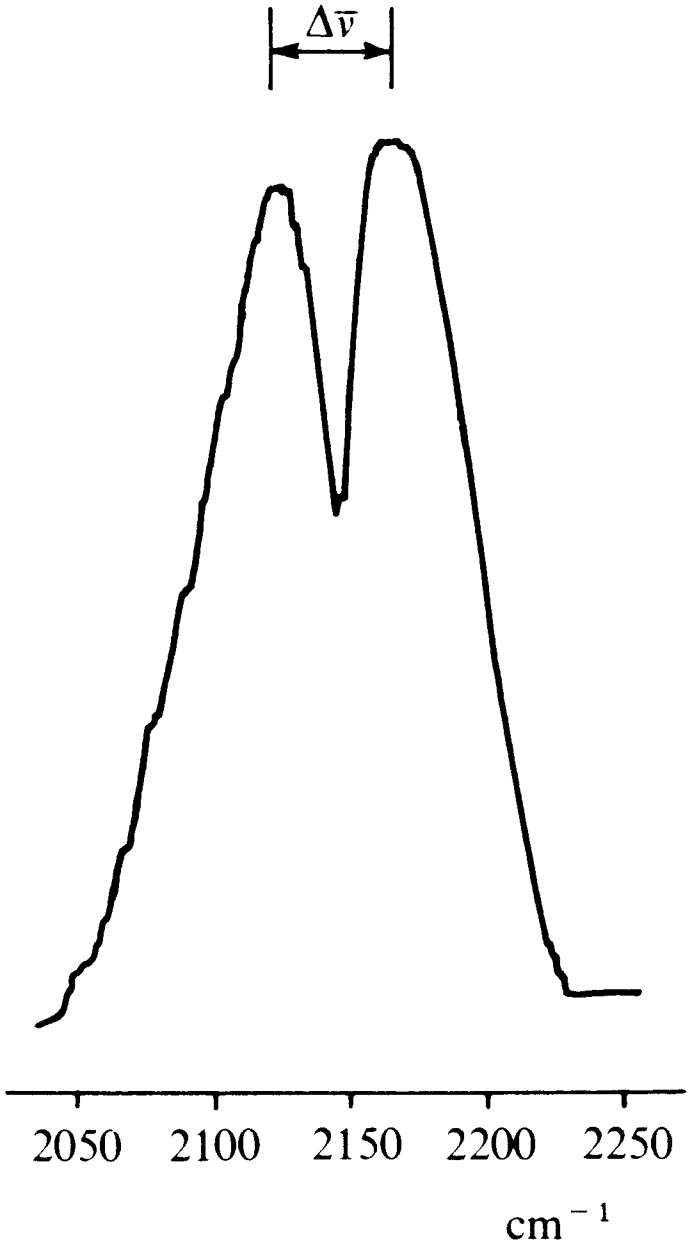

The fundamental band of carbon monoxide under very low resolution. All rotational fine structure is lost and a PR contour is observed.

Figure 2.31 Fundamental band of carbon monoxide under very low resolution.

equally spaced bands with a spacing of 2B on each side of the band origin $\tilde{\nu}_0$. Since m cannot be zero, the band origin itself will not appear. Lines to the low frequency side of $\tilde{\nu}_0$ are referred to as the P-branch, while those to the high frequency side are called the R-branch.

The influence of rotation on the spectra of polyatomic molecules.

We described that the selection rules of diatomic molecules for a simultaneous rotation and vibration were given by

$$\Delta v = 0,\ \pm 1,\ \pm 2,\ \pm 3\ \ldots.\ ;\quad \Delta J = \pm 1,\ \Delta J \neq 0$$

and that this gave rise to a spectrum consisting of approximately equally spaced line series on each side of a central minimum, designated as the band center.
We now consider molecules with more than two atoms. We can divide the possible vibrations of complex molecules into those causing a dipole change either (1) parallel or (2) perpendicular to the major axis of rotational symmetry. The purpose of this distinction is that the selection rules depend on the type of vibration, parallel or perpendicular, which the molecule is undergoing (see Figure 2.32 below, a diatomic molecule can only have parallel vibrations):

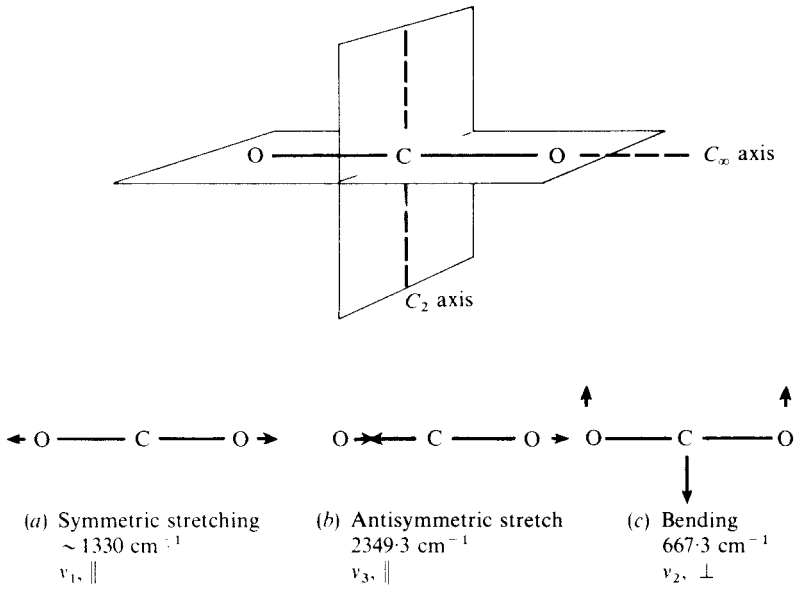

The symmetry and fundamental vibrations of the carbon dioxide molecule.

Figure 2.32 Symmetry and fundamental vibrations of the carbon dioxide molecule.

As a simple case, we consider a linear molecule of three atoms. Parallel vibrations have selection rules that are identical with those for diatomic molecules.

$$\Delta J = \pm 1,\ \Delta v = \pm 1 \text{ for harmonic vibrations}$$

and

$$\Delta J = \pm 1,\ \ \Delta v = \pm 1, \pm 2, \pm 3, \ldots \text{ for anharmonic vibrations}$$

The spectrum of a parallel vibration will thus be similar in appearance to that of a diatomic molecule (see the parallel stretching vibration of the HCN molecule in Figure 2.33).

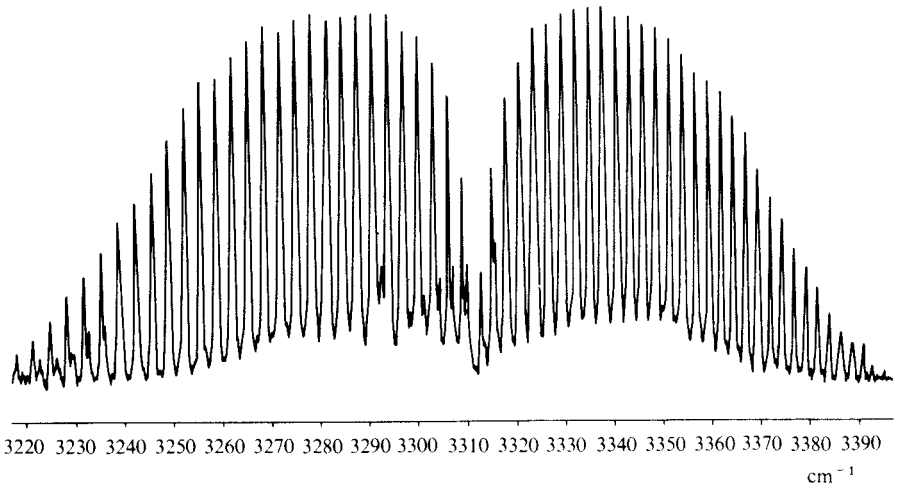

Figure 2.33 Spectrum of the symmetric stretching vibration of the HCN molecule.

Perpendicular vibrations. For these the selection rule is found to be

$$\Delta v = \pm 1,\ \ \Delta J = \ 0, \pm 1 \text{ for simple harmonic motion}$$

This implies for the first time, that a vibrational change can take place with no simultaneous rotational transition. The result is depicted in Figure 2.34 below, which shows the same energy levels and transitions as a linear diatomic molecule, with the addition of ΔJ=0 transitions. If the oscillation is taken as simple harmonic, the energy levels are identical with those previously given:

$$\varepsilon_{total} = \varepsilon_{j,v} = BJ(J+1) + \left(v + \frac{1}{2}\right) c\tilde{\nu}_{vib} - x\left(v + \frac{1}{2}\right)^2 c\tilde{\nu}_{vib}$$

with the corresponding P and R branch lines.

Transitions with a ΔJ=0, however, correspond to a Q-branch whose lines are derived from the equation:

$$\begin{aligned}\Delta\varepsilon_{v,J} &= \varepsilon_{J+1,v+1} - \varepsilon_{J,v} \\ &= 1\frac{1}{2}\tilde{\nu}_e - 2\frac{1}{4}x_e\tilde{\nu}_e + BJ(J+1) - \left\{\frac{1}{2}\tilde{\nu}_e - \frac{1}{4}x_e\tilde{\nu}_e + BJ(J+1)\right\} \\ &= \tilde{\nu}_0 \quad (\text{in cm}^{-1}), \qquad \text{for all } J\end{aligned}$$

Thus the Q branch consists of lines superimposed upon each other at the band center $\tilde{\nu}_0$. One contribution arising from each of the populated J values gives usually a very intense line.
See diagram (Figure 2.34) and spectra (Figure 2.35) of the H-CN bending vibration below.

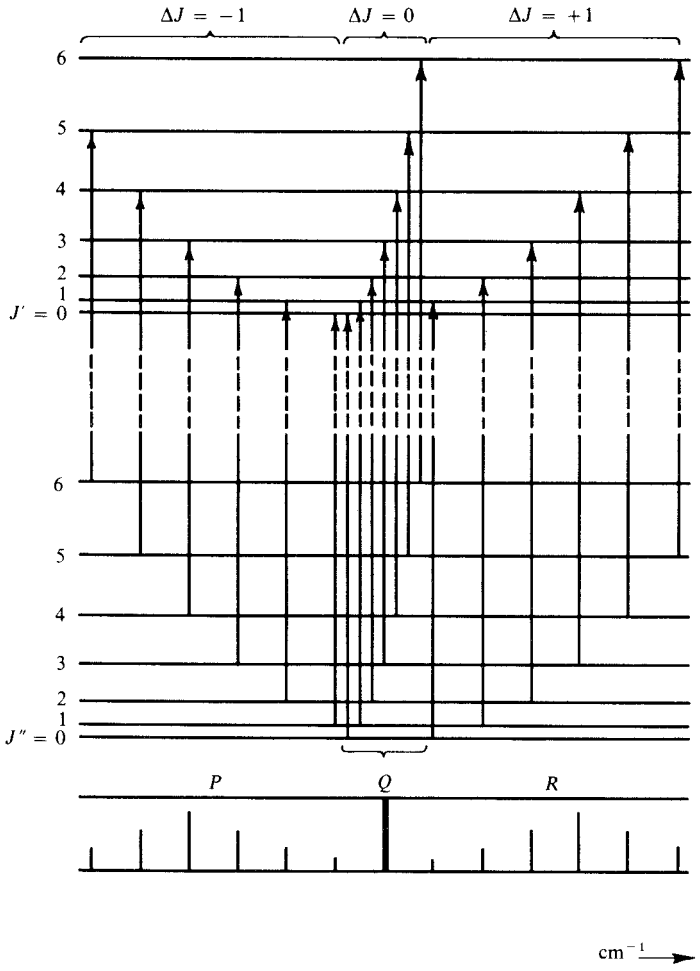

The rotational energy levels for two vibrational states showing the effect on the spectrum of transitions for which ΔJ=0.

Figure 2.34 Appearance of the Q branch in rotation-vibration spectra of the H-CN bending vibration.

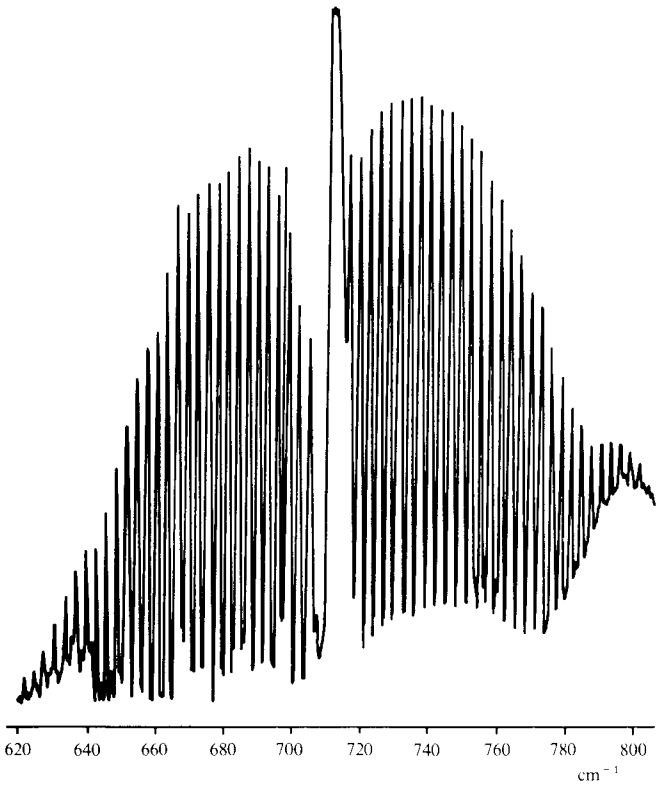

Spectrum of the bending mode vibration of the HCN molecule. The PQR structure of the spectrum becomes evident.

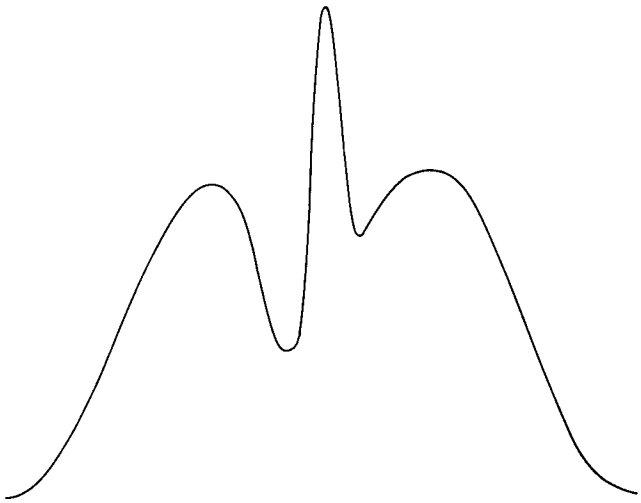

The contour of a PQR band under low resolution.

Figure 2.35 Rotation vibration spectrum of the bending vibration in an HCN molecule.

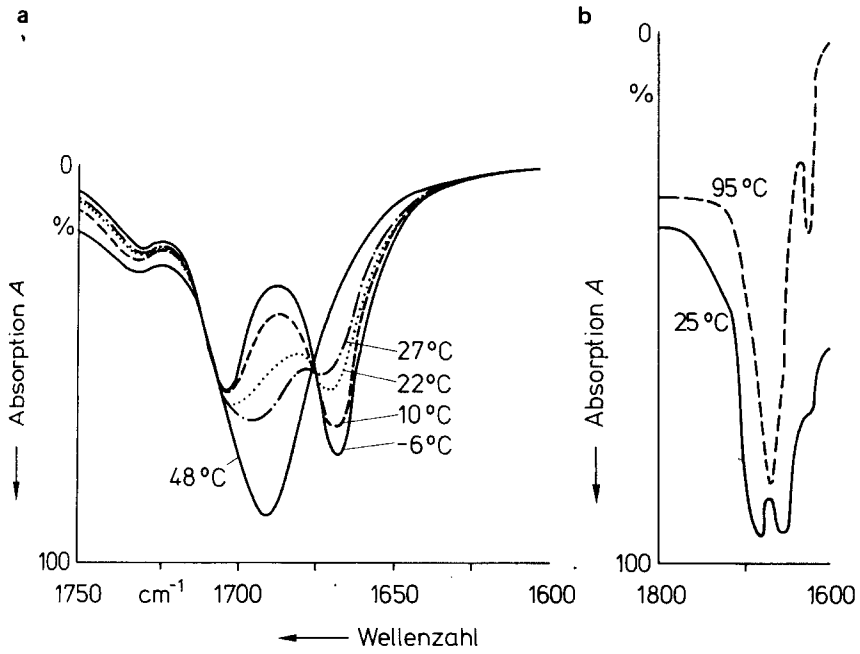

IR-spectra of a selected region of a, poly-cytidine/5-guanosine monophoshate and b, DNA as a function of temperature. (After Howard, F.B. et al. (1969), Proc. Nat. Acad. Sci., USA 64, 451 and after Kolkenbeck, K., Zundel, G. (1975), Biophysics Struct. Mech., 1, 203.)

Figure 2.36 IR spectra of polynucleotides.